

**KERNFORSCHUNGSZENTRUM
KARLSRUHE**

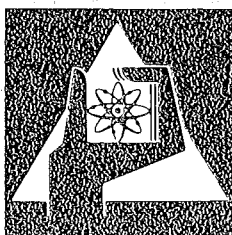
Juni 1976

KFK 2298

Institut für Angewandte Kernphysik

**Operation of the Karlsruhe Isochronous Cyclotron
in 1975**

F. Schulz, H. Schweickert



**GESELLSCHAFT
FÜR
KERNFORSCHUNG M.B.H.**

KARLSRUHE

Als Manuskript vervielfältigt

Für diesen Bericht behalten wir uns alle Rechte vor

GESELLSCHAFT FÜR KERNFORSCHUNG M. B. H.
KARLSRUHE

KERNFORSCHUNGSZENTRUM KARLSRUHE

Institut für Angewandte Kernphysik/Zyklotron

April 1976

KFK 2298

Operation of the Karlsruhe Isochronous Cyclotron
in 1975

F. Schulz, H. Schweickert

Gesellschaft für Kernforschung m.b.H., Karlsruhe

Zusammenfassung

Betrieb des Karlsruher Isochron Zyklotrons im Jahre 1975

Es wird ein kurzer Überblick über den Betrieb des Karlsruher Isochron Zyklotrons im Jahre 1975 gegeben. Die wesentlichen Gründe für eine kurze Wartungs- und Umbauperiode und einige technische Verbesserungen zur Erhöhung der Zuverlässigkeit der Beschleunigeranlage werden diskutiert. Ferner wird über den Status und die Ergebnisse einer Reihe von Weiterentwicklungen am Zyklotron berichtet:

Das axiale Einschußsystem

Die Rechnerunterstützung des Zyklotronbetriebes

Ionenquellenentwicklung

Berührungslose, kapazitive Strahlstrommessung

Neue Korrekturspulen für das Zyklotron

Verbesserung des Neutronenflugzeit-Spektrometers

Das wachsende Interesse Beschleuniger dieser Art für nichtkernphysikalische anwendungsorientierte Forschungsprobleme einzusetzen wird durch Kurzberichte der Experimentatoren aus folgenden Fachgebieten dokumentiert:

Festkörperphysik

Ingenieurtechnik

Materialforschung

Nuklearmedizin

Nuklearchemie

Abstract

The operation of the Karlsruhe Isochronous Cyclotron in 1975 is briefly surveyed. The main cause of one very short period for maintenance, repair and installation and several additional efforts to improve the reliability of the accelerator installation are discussed. The status and the results of several technical developments for the cyclotron are described:

The axial injection system

Computer aided cyclotron operation

Ion source development

Capacitive current measurement at the external beam

New correction coils for the cyclotron

Improvement of the neutron time-of-flight spectrometer

As there is an increasing interest in using this type of accelerator for research in fields other than nuclear physics, it was felt appropriate to present short surveys on investigations at our cyclotron in 1975 in the fields of:

Solid state physics

Engineering

Materials research

Nuclear medicine

Nuclear chemistry

TABLE OF CONTENTS

	Page
1. OPERATION SUMMARY	
F. Schulz, H. Schweickert	1
2. TECHNICAL DEVELOPMENTS	7
2.1 The Axial Injection System	
G. Haushahn, J. Möllenbeck, F. Schulz, H. Schweickert	7
2.2 Computer Aided Cyclotron Operation	
W. Kappel, W. Karbstein, W. Kneis, J. Möllenbeck, H. Schweickert	9
2.3 Ion Source Development	
J. Biber, H. Kuhn, F. Schulz	12
2.4 Capacitive Current Measurement at the External Beam	
G. Haushahn, K. Heidenreich, E. Röhrl	14
2.5 New Correction Coils for the Cyclotron	
G. Haushahn, J. Möllenbeck, Ch. Rämer, H. Schweickert, F. Schulz	15
2.6 Improvement of the Karlsruhe Fast Neutron Time-of-Flight Spectrometer	
S. Cierjacks, D. Erbe, K. Kari, B. Leugers, I. Schouky, G. Schmalz, F. Voss, G. Haushahn, K. Heidenreich, F. Schulz	18
3. NON-NUCLEAR PHYSICS AT THE CYCLOTRON	23
3.1 Solid State Physics	23
3.1.1 Hyperfine Interactions in Liquid Semi- conductors	
D. Quitmann, H. Hadijuana, W. v. Hartrott, J. Roßbach, E. Weihreter	23
3.1.2 Hyperfine Interactions of ^{197}Au and $^{197\text{m}}\text{Hg}$ in Various Metals Studied by the Mössbauer Effect and Time-Differential Perturbed- Angular-Correlations	
B. Perscheid, H. Büchsler, J.C. Soares, K. Freitag, M. Forker	26
3.1.3 Mössbauer Spectroscopy with ^{61}Ni	
G. Czjzek, J. Fink, H. Schmidt	28
3.1.4 The Hyperfine Field of Mercury in Iron	
K. Freitag, P. Herzog, P.K. James, N.J. Stone	31
3.2 Engineering	33
3.2.1 Thin Layer Radioactivation of Machine Components	
G. Essig, E. Rühl	33
3.2.2 Use of Cyclotron Activated Fluorine-18 in Investigations Relating to Process Engineering	
J. Schmitz, A. Merz	35

	Page
3.3 Nuclear Medicine	37
3.3.1 The Production of Radionuclides ^{123}I , ^{77}Br for Nuclear Medicine with High Energetic ^4He Particles F. Helus, W. Maier-Borst, R.M. Lambrecht, A.P. Wolf	37
3.3.2 Studies of Chemistry and Potential Nuclear Medical Application of ^{211}At K. Rössler, G.-J. Meyer, G. Stöcklin	45
3.3.3 Investigation of the Suitability of ^{125}Xe for Application in Nuclear Medicine S. Göring, A. Hanser, G. Haushahn, G. Schatz, W.E. Adam, F. Bitter, H. Kampmann	47
3.3.4 Potassium-43 Production F. Michel, H. Münzel	49
3.4 Materials Research	52
3.4.1 Helium Bath Irradiation Facility for Superconductors H. Becker, P. Maier, J. Pytlik, H. Ruoss, E. Seibt	52
3.4.2 Apparatus to Study Irradiation-Induced Creep with a Cyclotron K. Herschbach, K. Müller	57
3.4.3 Radiation Damage Experiments D. Kaletta, G. Przykutta	59
3.5 Nuclear Chemistry	61
3.5.1 Studies of the Independent Yields of $^{148\text{m}}\text{Pm}$ and $^{148\text{g}}\text{Pm}$ and their Isomer Ratio in α -Particle Induced Fission of ^{232}Th D.C. Aumann, W. Gückel, E. Nirschl, H. Zeising	61
3.5.2 Excitation Functions of ^3He -Reactions with Y and Nb S. Flach and H. Münzel	63
3.5.3 Model Experiments Concerning the Separation and Identification of Short-Lived Elements Specially with Regard to Transactinides W. Fröschen, I. Dreyer, G.K. Wolf	65
3.5.4 A Nondestructive Determination of P, Ca and K in Soil by Means of α -Particle Activation C.C. Dantas, P. Misaelides	70
PUBLICATIONS	73

1. OPERATION SUMMARY

F. Schulz, H. Schweickert

Institut für Angewandte Kernphysik/Zyklotron des
Kernforschungszentrums Karlsruhe

Within 1975 the machine was in full operation except for one very short shut-down period described below. The cyclotron was used for irradiations during 6824 hours, which amounts to 86.8 % of the total operating time and thus yielded the best result obtained since the existence of this accelerator facility. Table 1 presents a survey of cyclotron operation during the period of reporting. The axial injection system for experiments involving polarized deuterons (52 MeV) and high-energy ${}^6\text{Li}^{3+}$ ions (156 MeV) was used routinely for the first time. The 501 hours indicated for experiments (11 % of the total experimental time) were equally distributed to these two types of ions. The relatively longer unscheduled shut-downs during operation with the axial injection system are exclusively due to failures of the very complicated ion sources.

The reason for the short shut-down period of 4 days in August 75 was a breakdown of one of the power supplies for the correcting coils during an isotope production with 60 μA of protons in the internal beam. As this breakdown was not observed immediately by the operator the produced large axial oscillation results in a considerable amount of beam loss on the SW-correcting coil. The coil therefore was destroyed and had to be exchanged.

According to the failure statistics of the past years several additional efforts have been made:

- New CAMAC controlled trim-coil powersupplies have been installed
- Improved extraction elements have been machined (see Fig. 1)
- An additional cooling system which will be used for the new correcting coils and the axial injection line was completed.
- A new room for the irradiation of machine parts has been built.

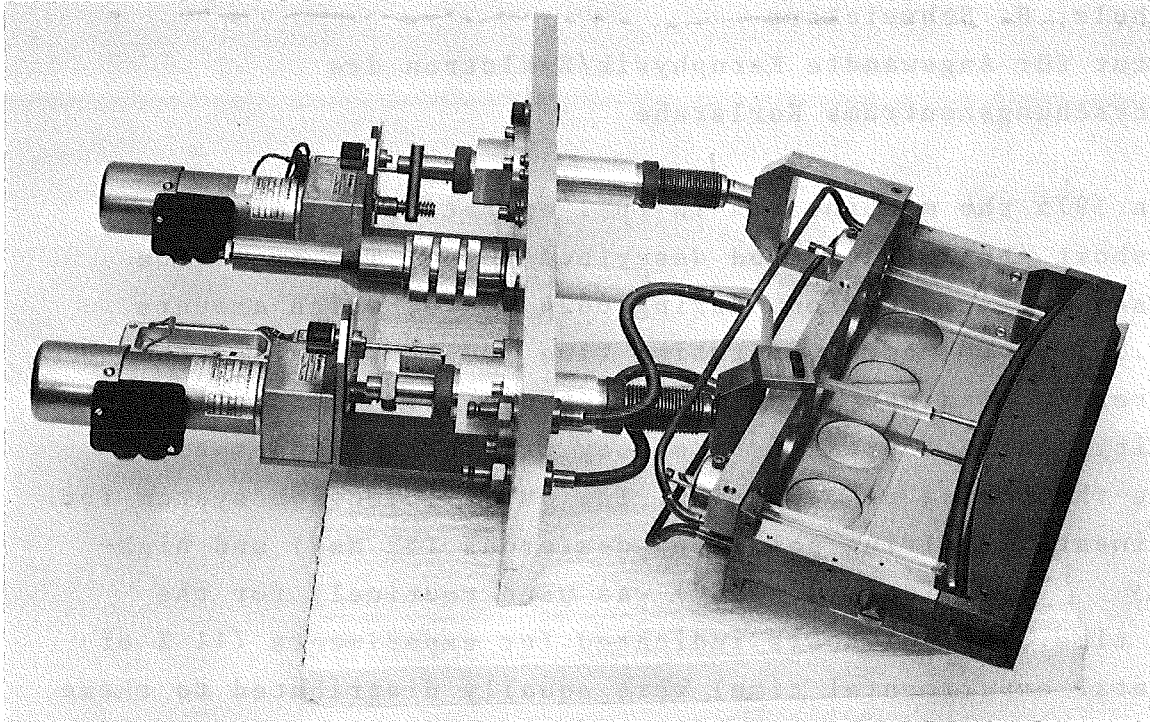


Fig. 1: One of the new extraction elements of the Karlsruhe Isochronous Cyclotron, which can stand approximately 1000 Watt beam power. All the parts, except the tantalum anti-septum, which can be seen by the beam are machined out of graphite

Tables 1 to 4 show the operational statistic 1975 in a form similar to that of the previous reports ¹⁻²⁾.

On the users' side (Table 3) the tendency observed for some years ²⁾ continues that the number of external (not GfK) experimentalists increases. The use of the cyclotron for application oriented research projects amounted to about 40 % of the total time of experimentation during the period of reporting.

References

- 1) G. Schatz, F. Schulz, KFK-Ext. 18/72-1
- 2) G. Schatz, F. Schulz, H. Schweickert, KFK-Ext. 18/75-1

Cyclotron operational	with internal ion sources		with external ion sources		total	
for experiments	5550 h	81.8 %	658 h	61.2 %	6208 h	79 %
for beam development and testing new components	390 h	5.8 %	225 h	20.9 %	615 h	7.8 %
Total time of operation	5940 h	87.6 %	883 h	82.1 %	6823 h	86.8 %
Scheduled shut-down for maintenance, repair and installation	365 h	5.3 %	54 h	5 %	419 h	5.4 %
Unscheduled shut-down	478 h	7.1 %	138 h	12.9 %	616 h	7.8 %
Total shift time	6783 h	100 %	1075 h	100 %	7858 h	100 %

Table 1: Operation of the Karlsruhe Isochronous Cyclotron in 1975

Cyclotron

Radiofrequency system	148 h	24.0 %
Axial injection including ion sources	138 h	22.4 %
Internal ion sources	80 h	13.0 %
Vacuum system (including all leaks)	57 h	9.3 %
Extraction	37 h	6.0 %
Magnet power supplies	18 h	3.0 %
Others	17 h	2.7 %
	<hr/>	<hr/>
Cyclotron total	495 h	80.4 %

Additional equipment

Targets (including target transport, cooling, automatic target handling)	66 h	10.7 %
Internal deflector for neutron time-of-flight experiments	26 h	4.2 %
External beam handling system	18 h	3.0 %
Safety control system	3 h	0.5 %
	<hr/>	<hr/>
Additional equipment total	113 h	18.4 %
Loss of machine time due to high radiation level	7 h	1.2 %
	<hr/>	<hr/>
Grand total	615 h	100 %

Table 2: Main causes of unscheduled shut-down in 1975

GfK - Karlsruhe users

Institut für Angewandte Kernphysik	1720 h	27.6 %
Labor für Isotopentechnik	910 h	14.7 %
Institut für Experimentelle Kernphysik	338 h	5.5 %
Institut für Radiochemie	298 h	4.8 %
Institut für Material- und Festkörperforschung	202 h	3.3 %
Institut für Heiße Chemie	89 h	1.4 %
	<hr/>	<hr/>
	3557 h	57.3 %

External users

Freie Universität Berlin	781 h	12.6 %
Max-Planck-Institut für Kernphysik, Heidelberg	490 h	7.9 %
Universität Heidelberg	338 h	5.4 %
Universität Erlangen	290 h	4.7 %
Universität Mainz	267 h	4.3 %
Technische Universität München	164 h	2.7 %
Kernforschungsanlage Jülich	89 h	1.4 %
Deutsches Krebsforschungszentrum, Heidelberg	77 h	1.2 %
Universität Bonn	71 h	1.1 %
Universität Hamburg	48 h	0.8 %
Universität Giessen	20 h	0.3 %
Universität Saarbrücken	16 h	0.3 %
	<hr/>	<hr/>
	2651 h	42.7 %

Grand total 6208 h 100 %

Table 3: User statistic for 1975

Nuclear reactions	1963 h	31.6 %
Solid state physics	1190 h	19.2 %
Engineering	911 h	14.7 %
Nuclear spectroscopy	798 h	12.8 %
Materials research	436 h	7.0 %
Nuclear medicine	316 h	5.1 %
Neutron physics	307 h	4.9 %
Nuclear chemistry	239 h	3.8 %
Others	48 h	0.9 %
	<hr/> 6208 h	<hr/> 100 %

Table 4: Users statistics for 1975

Period	Numbers of persons	Total dose (man-rem)	Mean dose (rem)
1968	12	8.77	0.73
1969	18	27.98	1.55
1970	18	33.83	1.88
1971	15	21.61	1.44
1972	15	16.06	1.07
1973	15	19.27	1.28
1974	15	16.22	1.08
1975	14	15.11	1.08

Table 5: Total radiation dose received by operating personnel

2. TECHNICAL DEVELOPMENTS

2.1 The Axial Injection System

G. Haushahn, J. Möllenbeck, F. Schulz, H. Schweickert
Institut für Angewandte Kernphysik/Zyklotron des
Kernforschungszentrums Karlsruhe

An extensive paper on this development until June 75 has been presented at the 7th Int. Conf. on Cyclotrons in Zürich ¹⁾. Therefore we can be brief and give here only a short summary. Since late 1974 both ion sources, the Lambshift ion source for polarized deuterons and the ${}^6\text{Li}^{3+}$ Penning source, have been installed in a basement room of the experimental hall (Fig. 1). The 12 m long horizontal electrostatic beam guide up to the 90° deflector did not entail additional difficulties. It allows access to the sources during isotope production periods at the internal beam and during optimization work at the injection system (Fig. 2).

The maximum beam currents obtained so far are listed in Table 1.

	Internal Beam Current	External Beam Current
Polarized d (52 MeV)	100 nA	40 nA
${}^6\text{Li}^{3+}$ (156 MeV)	10 nA	5 nA

Table 1: Maximum beam currents with the Karlsruhe injection system

Reference

- 1) G. Haushahn, J. Möllenbeck, G. Schatz, F. Schulz, H. Schweickert; Proc. 7th Int. Conf. on Cyclotrons and their Applications (Birkhäuser, Basel, 1975). p. 376-380

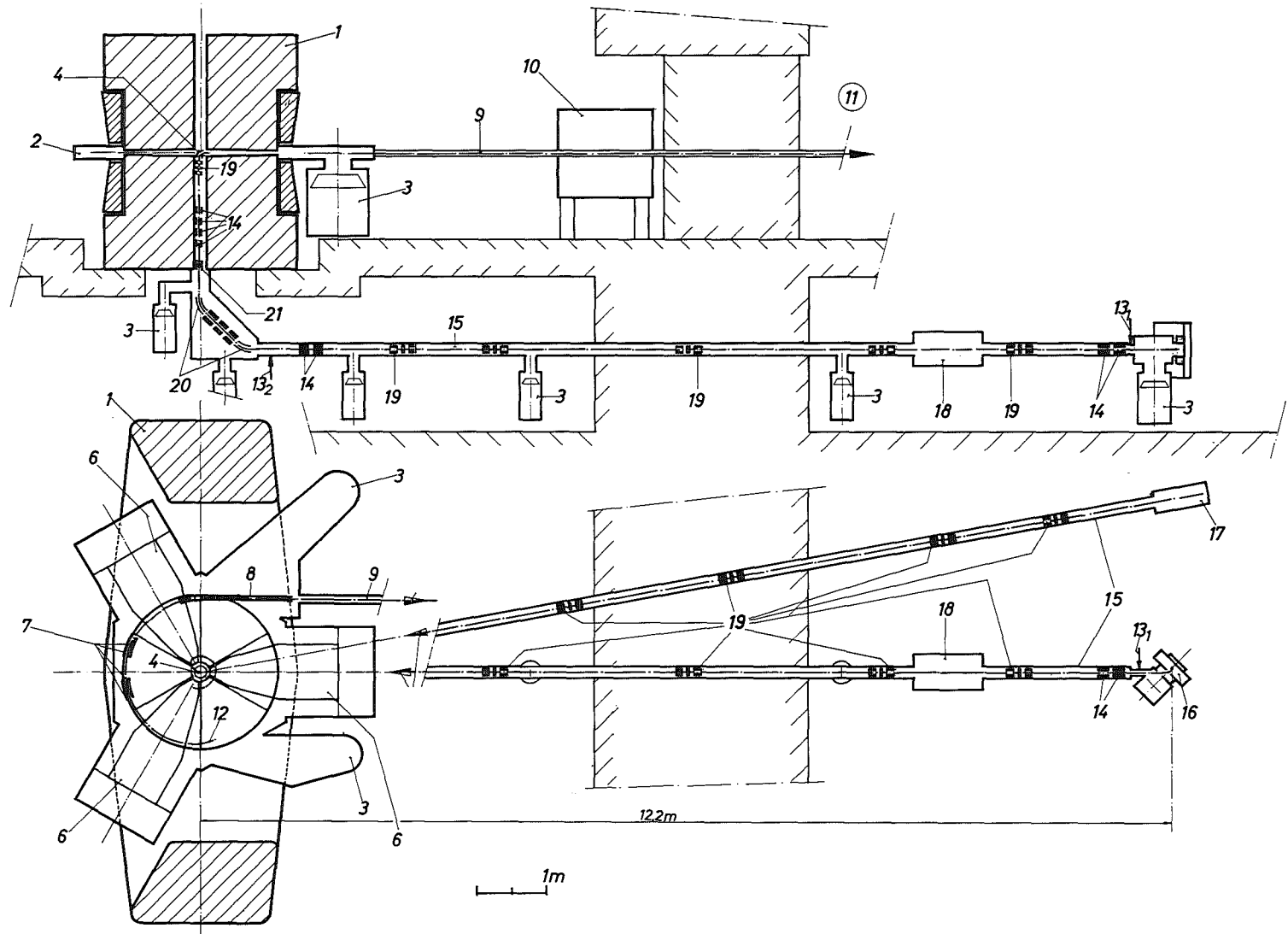


Fig. 1: Schematic cross-sections of the Karlsruhe axial injection system. 1: cyclotron magnet; 2: vacuum chamber; 3: diffusion pumps; 4: hyperboloid inflector; 6: accelerating system; 7: electric extraction elements; 8: magnetic channel; 9: high energy beam line; 10: switching magnet; 11: experimental hall; 13: beam stop; 14: electrostatic quadrupoles; 15: horizontal line; 16: ${}^6\text{Li}^{3+}$ ion source; 17: Lambshift ion source; 18: emittance measurement set up; 19: einzel lenses; 20: 90° bending element; 21: buncher

2.2 Computer Aided Cyclotron Operation

W. Kappel, W. Karbstein, W. Kneis, J. Möllenbeck, H. Schweickert
Institut für Angewandte Kernphysik/Zyklotron des Kern-
forschungszentrums Karlsruhe

To adapt the machine to frequently changing user requests, the operators need fast and reliable measurements of parameters capable of optimization. These tasks can be carried out in an almost ideal way by on-line computer. The main advantages it offers are rapidity, reliability and reproducibility of the measurements. Moreover, complicated measurement processes and their evaluation can be performed by the operators.

In May 75 a new computer configuration (Fig. 1) consisting of a NOVA 2/10 with 32K core memory, two disks, two terminals and a CAMAC branch controller has been installed. A parallel CAMAC branch of 200 m length interconnects the 5 crates in the control room, in the experimental hall and in the cyclotron vault. The costs of the computer system up to the first CAMAC crate amount to DM 100.000.

The common language used for all measurement programs is BASIC which is running under the RDOS disk operating system. A number of assembler subprograms are available for CAMAC I/O, which can be called from BASIC via CALL statements. All measurement programs have been grouped into a measurement program system named CICERO consisting of a number of measuring programs and the respective tables (Fig. 2).

In addition to the "status cyclotron" and "status external beam" programs also the "emittance external beam" and "phase width internal" programs are ready for operation (Fig. 3 and 4). A number of relevant cyclotron parameters are measured with the "status" programs. The operational modes "adjustment" and "drift test" of single parameters are particularly useful in this context. The phase width and the emittance can be measured by the operators within 10 and 60 s, respectively ¹⁾.

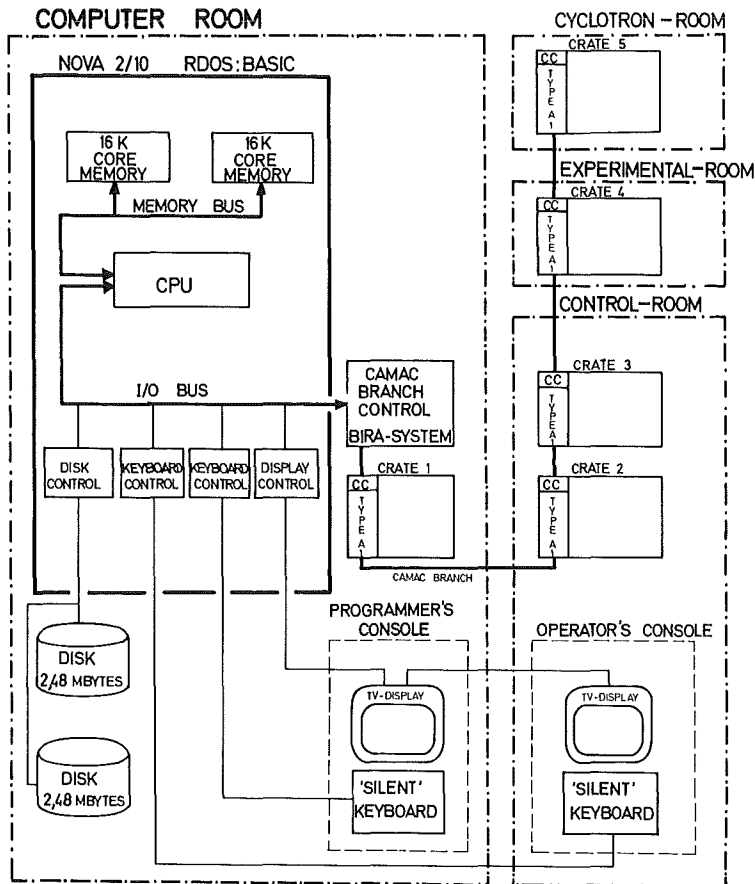


Fig. 1: Computer configuration in support of cyclotron operation, consisting of a NOVA 2/10 with 32K core memory, 2 disks, 2 terminals and a CAMAC branch controller. The measured data are digitalized in situ and transmitted to the computer via a 200 m CAMAC branch highway

 CICERO TABLE PAGE 1

Fig. 2: List of measurement programs ready for use as displayed on the television screen in the control room. By input of a number the cyclotron operator selects the diagnostics program required. The computer subsequently executes this program and displays the result on the television screen.

- 0 - PHASE WIDTH INTERNAL
- 1 - PHASE WIDTH EXTERNAL
- 2 - PHASE POSITION $\Phi = f(R)$
- 3 - EMITTANCE EXTERNAL BEAM
- 4 - STATUS EXTERNAL BEAM
- 5 - STATUS CYCLOTRON
- 6 - DIFF. TARGET R=100-1040
- 7 - AXIAL TARGET R=100-1040
- 8 - ABS. ENERGY MEASUREMENT
- 9 - CONTR. OF PULSING SYSTEM

 'RET' - NEXT PAGE
 - - - - - PREVIOUS PAGE
 Z - BACK TO CICERO

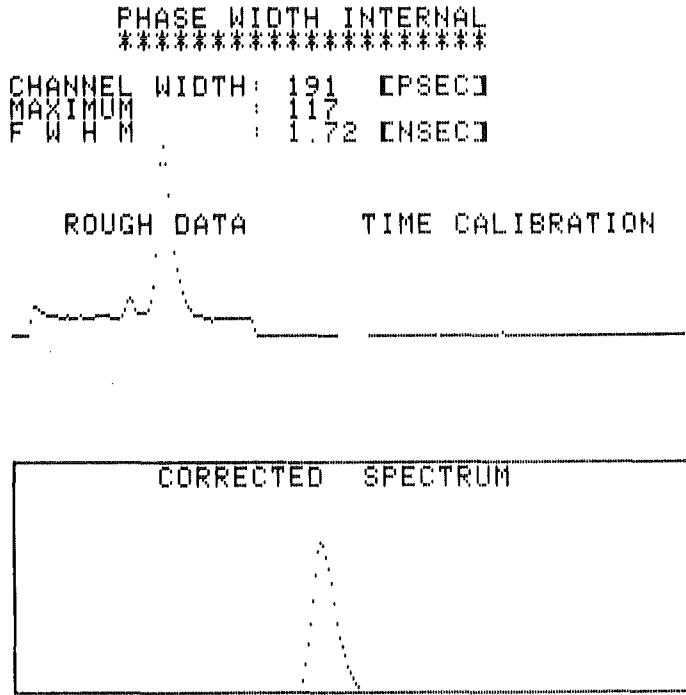


Fig. 3: Result of a phase width measurement of the internal beam performed by the computer. Before the measurement starts the computer carries out an automatic time calibration. 10 seconds are needed from the start of measurement until the display of the television picture shown in this figure.

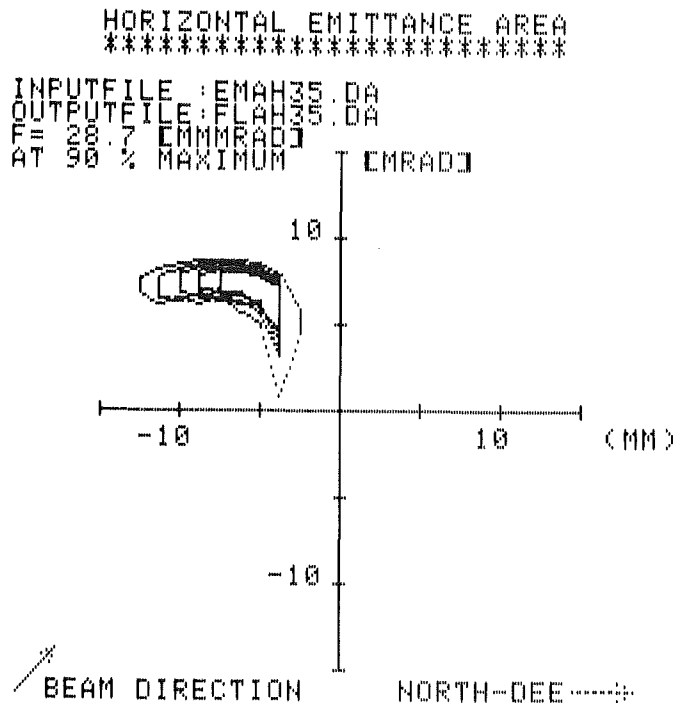


Fig. 4: Result of an emittance measurement performed by the computer at the extracted 52 MeV deuteron beam. Via CAMAC the computer controls the mechanical and electronic units necessary and accepts the raw data. It calculates from these data the emittance area shown on the screen. The result clearly shows the deviations of the extracted beam from the optical axis of the beam guiding system with respect to location and direction

References

- 1) W. Kappel, W. Karbstein, W. Kneis, J. Möllenbeck, D. Hartwig, G. Schatz, H. Schweickert; Proc. 7th Int. Conf. on Cyclotrons and their Applications (Birkhäuser, Basel, 1975) p. 538-541

2.3 Ion Source Development

J. Biber, H. Kuhn, F. Schulz

Institut für Angewandte Kernphysik/Zyklotron des
Kernforschungszentrums Karlsruhe

Ion source development was mainly directed towards improving the reliability of the external ${}^6\text{Li}^{3+}$ source such that it could be used in routine operation. The second cathode to be installed originally was substituted by a tantalum reflector connected with the cathode potential. Fig. 1 shows the configuration of this source. By use of the hafnium carbide cathode ¹⁾ (instead of tungsten) the lifetime of the source was extended by a factor 4. To achieve long lifetimes the source has also been operated at low arc power ($U_B = 250$ V, $I_B = 1.2$ A). In this operational mode the source yields $0.1 - 1 \mu\text{A}$ ${}^6\text{Li}^{3+}$ ions at an average life of 30 hours. Investigations conducted in a test bench have shown that the same source produces a 2 - 3 times higher yield of ${}^6\text{Li}^{3+}$ ions with higher magnetic fields (6 - 8 kG).

References

- 1) G. Schatz, F. Schulz; KFK-Ext. 18/73-1 (1973)

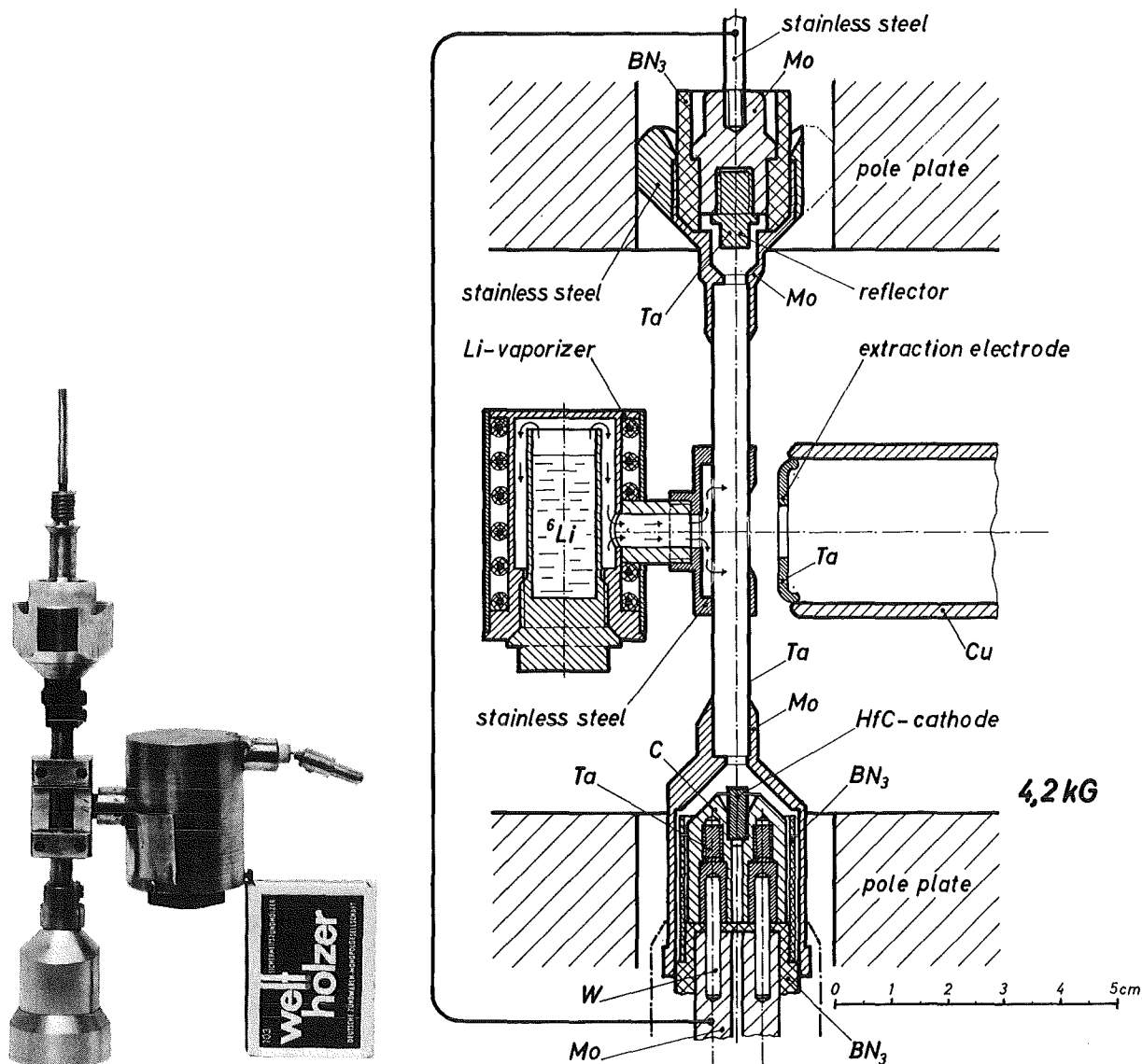


Fig. 1: Configuration of the ${}^6\text{Li}^{3+}$ Penning source. The lithium atoms are carried by the evaporator into a plasma established between the cathode and the reflector. Strong compression of this plasma by a homogeneous magnetic field of 5 kG is decisive for the production of the high-charge lithium ions.

2.4 Capacitive Current Measurement at the External Beam

G. Haushahn, K. Heidenreich, E. Röhr1

Institut für Angewandte Kernphysik/Zyklotron des Kernforschungszentrums
Karlsruhe

It is desirable for a number of applications at the cyclotron to measure the accelerated particle current in a capacitive mode, i.e. without intercepting. Measurement of low currents is made difficult by pick-up from the accelerating rf. We developed a configuration avoiding this difficulty by filtering the 2nd harmonic from capacitive pick-up signal. Our cyclotron beam is made up of ion pulses of about 1 - 3 ns width with a repetition frequency of 33 MHz. The charge introduced by such an ion bunch amounts to $1/2 I\tau$ (I =pulse amplitude,

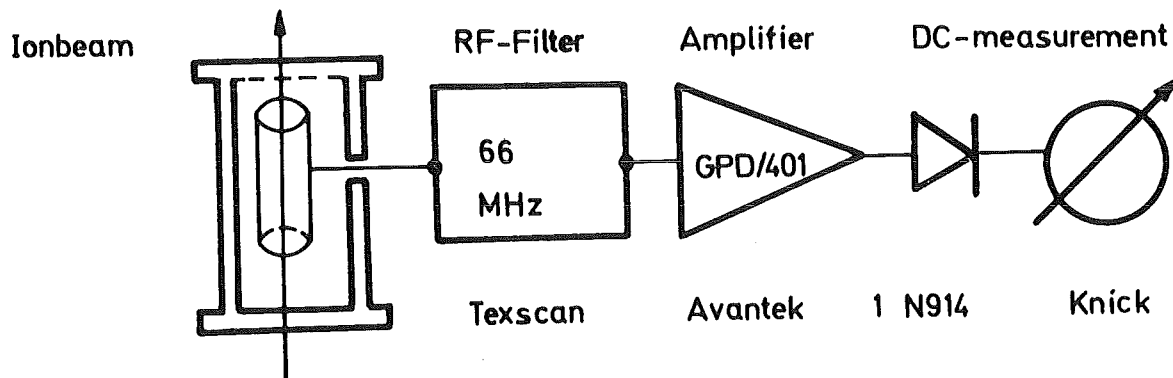


Fig. 1: Configuration for non-intercepting beam current measurement at the external cyclotron beam. Only the 2nd harmonic of the pick-up signal from the beam pulses is filtered out and processed further. This avoids disturbance of the measurement by interference of the acceleration frequency. Beam currents of 10 nA - 10 μ A can be measured very reliably with this unit

τ = pulse duration) with the charge pulses supposed to be triangular. If such a pulse shape is given in the form of a Fourier series it can be stated that for a small pulse duty factor $\alpha = \tau/T$ (T = pulse spacing) the first harmonics have roughly identical amplitudes ^{1,2)}

The block diagram of the electronic system used has been represented in Fig. 1. Beam currents of 10 nA - 10 μ A can be measured very reliably with this unit. Experiments to incorporate the capacitive probe into a 66 MHz oscillator circuit did not substantially improve the sensitivity. Presently a configuration is tested which is based on the same philosophy for the internal beam. This unit is intended to indicate the extraction rate in a non intercepting manner.

References

- 1) S.S. Sherman, R.G. Roddick, A.J. Metz, IEEE Trans. Nucl. Sci. NS-15 (1968) 500
- 2) R. Reimann, 153. Session Annuelle de la Société Helvétique des Sciences Naturelles. Lugano, Switzerland, Oct. 19-20 (1973)

2.5 New Correction Coils for the Cyclotron

G. Haushahn, J. Möllenbeck, Ch. Rämer, H. Schweickert, F. Schulz
Institut für Angewandte Kernphysik/Zyklotron des Kernforschungszentrums Karlsruhe

It is expected that the correction coil system of our cyclotron, must be replaced by a new one in 1977. Therefore, measurements and calculations were carried out in the last year, which centered around the question whether with a suitably modified correction coil arrangement $^3\text{He}^{2+}$ ions can be accelerated up to the extraction radius. This is possible in principle with

our fixed frequency machine by reducing the isochronous field to $3/4$ of the magnetic field value for $e/m = 1/2$ particles.

But reduction of the excitation current induces a change in the radial dependence of the magnetic field (see Fig. 1). Plot 1 represents the measured radial magnetic field distribution for $e/m = 1/2$ particle. Plot 3 shows the measured radial magnetic field distribution for which the resonance condition for $e/m = 2/3$ particle is fulfilled in the central zone. The deviation from the nominal value plot for ${}^3\text{He}^{2+}$ reaches up to 2 kG near extraction radius. Detailed calculations ^{1,2)} and measurements have now shown that field adaption for ${}^3\text{He}^{2+}$ and $e/m = 1/2$ ions is possible by the following modifications:

1. Removal of the outer shim to reduce the necessary maximum field correction from 2 kG to 1.2 kG.
2. Installation of a new summing correction coil system (cf. Figs. 2,3).

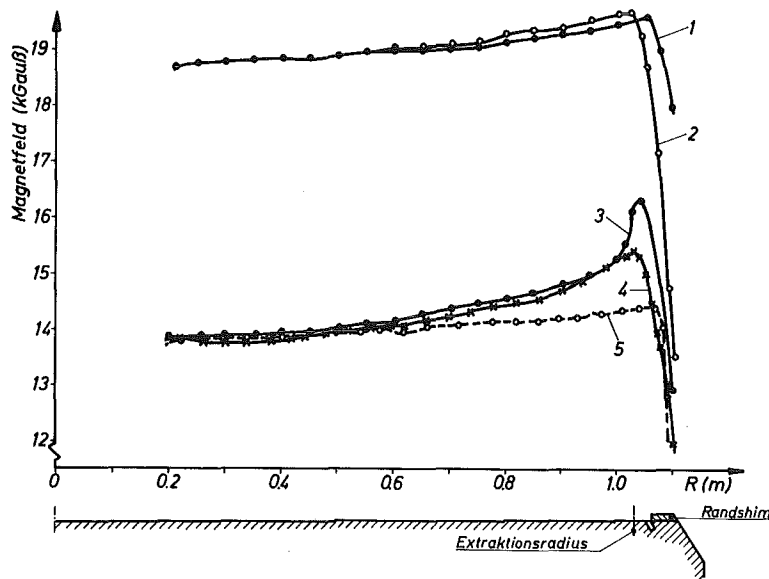


Fig. 1: Radial magnetic field distribution measured in the central plane of a strong sector. 1: Field plot for $e/m = 1/2$ particle; 2: Field plot for $e/m = 1/2$ particle without iron shim; 3: Field plot for $e/m = 2/3$ particle; 4: Field plot for $e/m = 2/3$ particle without iron shim; 5: Nominal field for $e/m = 2/3$ particle

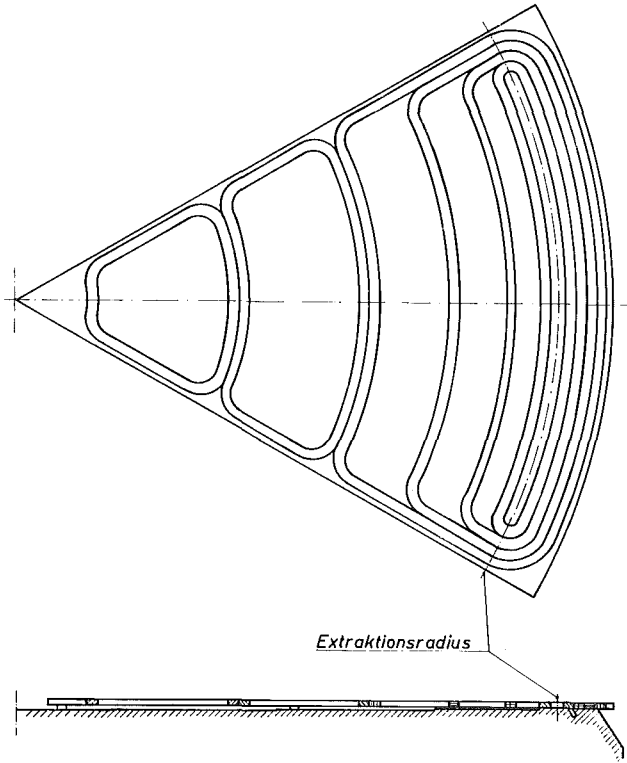


Fig. 2: New correction coil configuration allowing magnetic field shaping for ${}^3\text{He}^{2+}$ ions. The number of turns of the four outer summing coils lies between 20 and 60 for excitation currents up to 40 A. The location of the individual coils and the necessary field strength for compensation were determined with a fitting program

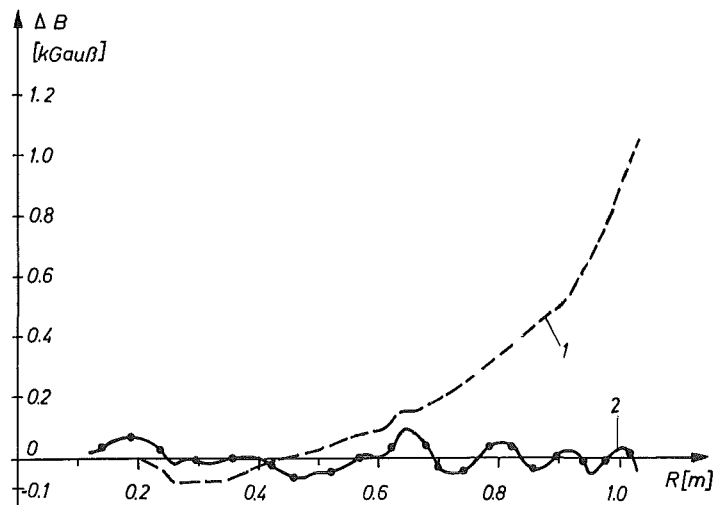


Fig. 3: Calculated field correction by the new correction coil configuration. 1: Field deviation for ${}^3\text{He}^{2+}$ ions without correction coils; 2: Field deviation with the coil configuration represented in Fig. 2

A prototype coil is under construction and will be available for test measurements by the middle of 1976. Installation of the new correction coil arrangement cannot be expected before the middle of 1977.

References

- 1) H. Braun; Die numerische Berechnung von Trimmspulfeldern, SIN-TM-03-13, 1970
- 2) G.W. Schweimer, (1973) unpublished

2.6 Improvement of the Karlsruhe Fast Neutron Time-of-Flight Spectrometer

S. Cierjacks, D. Erbe, K. Kari, B. Leugers, I. Schouky, G. Schmalz, F. Voss
Institut für Angewandte Kernphysik
G. Haushahn, K. Heidenreich, F. Schulz
Institut für Angewandte Kernphysik/Zyklotron des Kernforschungszentrums
Karlsruhe

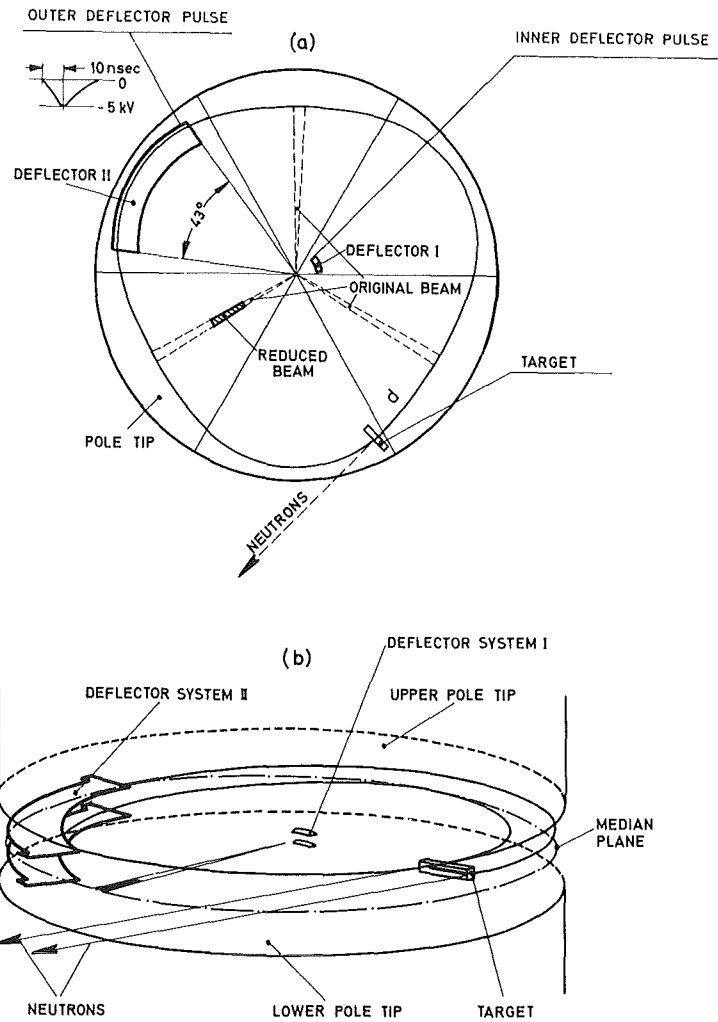
In order to carry out neutron time-of-flight experiments with the Karlsruhe cyclotron it is necessary to reduce the normal pulse repetition rate of 33 MHz. The reduction is accomplished by two coupled electrostatic deflector assemblies forming the 'deflection bunching' system. A scheme of this system is shown in fig. 1.

In normal continuous operation of the Karlsruhe cyclotron three microstructure pulses are delivered from the source since acceleration is accomplished in the third harmonic mode. This gives rise to a beam distribution which is indicated by the three regions between the dotted lines. The deflector system which is located near the center of the machine (deflector I) is used for a twofold purpose:

- (i) to eliminate two out of three microstructure pulses by deflection to a beam stop and

Fig. 1: Scheme of the bunching deflection system.

(a) Top view,
(b) Schematic drawing



(ii) to form packets of 4.5 μ sec duration (each consisting of 50 microstructure pulses) with a repetition rate up to 200 kHz.

As a result of this kind of deflection only the portion of the beam indicated by hatching will remain.

Both these objectives have been achieved with a suitable combination of the radial and an axial electrostatic deflector provided with an appropriate sinusoidal deflection voltage superimposed on a square wave high voltage pulse. This is illustrated in fig. 2. The upper curve shows the normal pulse structure at the position of the inner deflector plates (deflector I). If a deflection voltage of the form shown in the next lower curve is supplied to a radial deflector only every third microstructure pulse will pass this system because the voltage then is decreased to zero. The formation of the ion packet

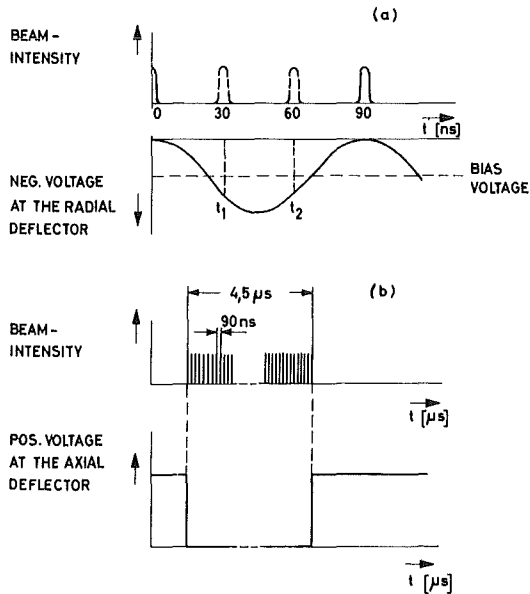


Fig. 2: Voltages of the deflector plates illustrating the principle of beam suppression. (a) Elimination of "two out of three" ion bunches. (b) Production of 4.5 μ sec pulses

is illustrated in the lower two curves of fig. 2. The bottom curve shows the deflection voltage which is supplied to an additional axial deflector. Since the deflection voltage decreases to the zero level for 4.5 μ sec only once during the pulse recurrence cycle, an ion packet as shown in the curve above is formed.

The subsequent procedure with the remaining beam is analogous to the treatment of beam deflection for neutron time-of-flight experiments in synchro-cyclotrons: A second axial deflector (deflector II of fig. 1) is located at the maximum radius of the machine with the plates above and below the medium plane of the cyclotron. This deflector serves to simultaneously deflect the whole set of microstructure pulses to a neutron producing target positioned above the medium plane of the cyclotron (see fig. 1b). At the time of deflection, the entire packet which is distributed over 10 cm in radius must be completely inside the area covered by the deflection plates. Before striking the target the deflected beam completes almost an additional orbit.

It is evident from this description that such a procedure produces single neutron pulses of the same pulse duration as the microstructure pulses, that is ~ 1 nsec, but increases the intensity in the neutron burst by almost a factor of 50.

Performance of Neutron Spectrometer

For neutron production a 3 mm thick natural uranium target is used. A typical unmoderated time-of-flight spectrum is shown in fig. 3. The broad maximum peak near 18 MeV is due to neutrons from deuteron break-up processes. The flat distribution at energies below ~ 6 MeV originates mainly from evaporation and fission processes. It is apparent from this illustration, that the useful energy range for measurements is between several hundred keV and ~ 30 MeV.

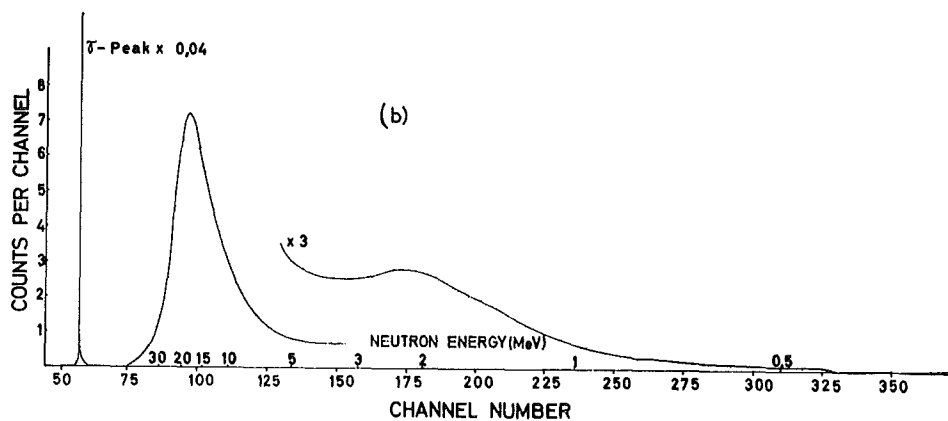


Fig. 3: Typical neutron time-of-flight spectrum

Today there are three different flight paths available. The first one at 12 m was built for investigations where a high neutron intensity but only moderate neutron energy resolution is required e.g. for the measurement of (n,x) cross sections and total fission cross sections of highly radioactive isotopes (^{239}Pu , ^{240}Pu). If a better energy resolution is necessary, measurements can be made at the 57 m or the 190 m flight path. The specifications of the different flight paths are shown in table 1. The values of the integrated neutron flux belong to a target current of 20 μA ; the energy resolution to a total time uncertainty of 3 nsec.

The main improvements of the last years have been on the one hand the increase in the maximum frequency for the pulsgenerators for the inner and outer deflectors from 20 kHz up to 200 kHz and on the other hand an increase in the maximum available deuteron source current from 100 μA up to 1 mA.

Flight Path	12 m	57 m	190 m
max. Repetition rate	200.000 pps	160 000 pps	30.000 pps
Integrated neutron flux at the detector in neutrons/cm ² · sec	$7.4 \cdot 10^6$	$3.3 \cdot 10^5$	$3.0 \cdot 10^4$
<u>Typ. energy resolution</u>			
at 1 MeV	7.1 keV	1.5 keV	0.4 keV
at 10 MeV	222.3 keV	46.8 keV	14.0 keV
at 20 MeV	632.4 keV	133.1 keV	39.9 keV
at 30 MeV	1169.8 keV	246.3 keV	73.9 keV

Table 1: Specifications of the Karlsruhe fast neutron time-of-flight spectrometer

To illustrate the capability of the spectrometer the high resolution total neutron cross section of iron between 0.5 and 0.9 MeV is shown in fig. 4.

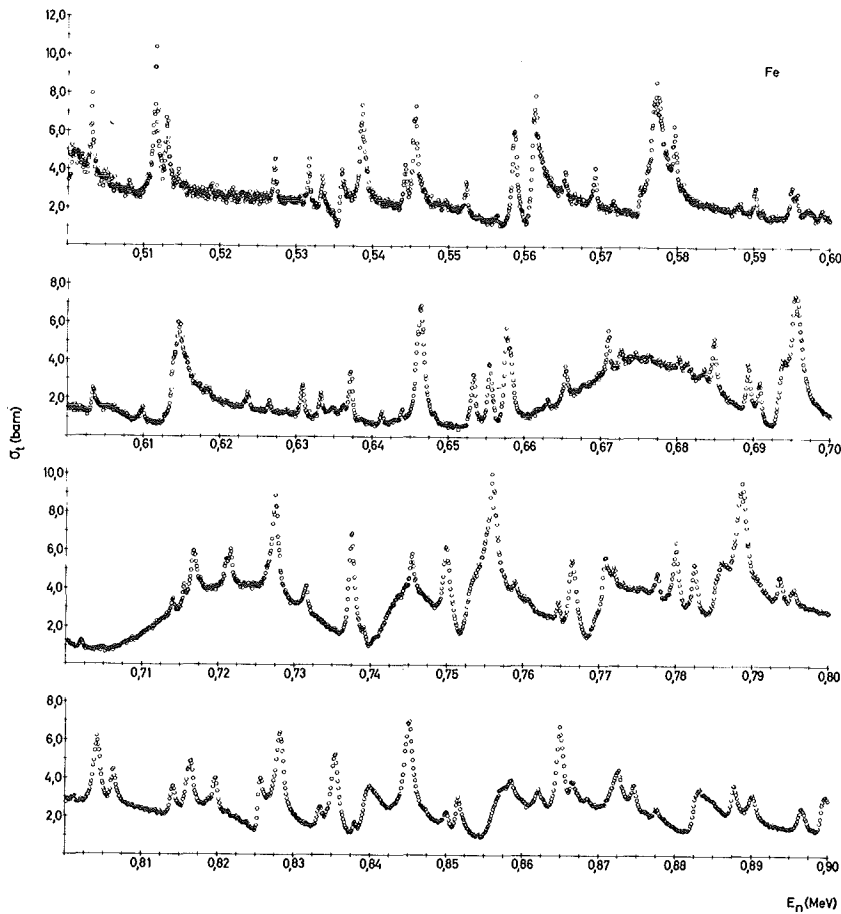


Fig. 4: Total neutron cross section of natural iron between 0.5 and 0.9 MeV

3. NON-NUCLEAR PHYSICS AT THE CYCLOTRON

3.1 Solid State Physics

3.1.1 Hyperfine Interactions in Liquid Semiconductors

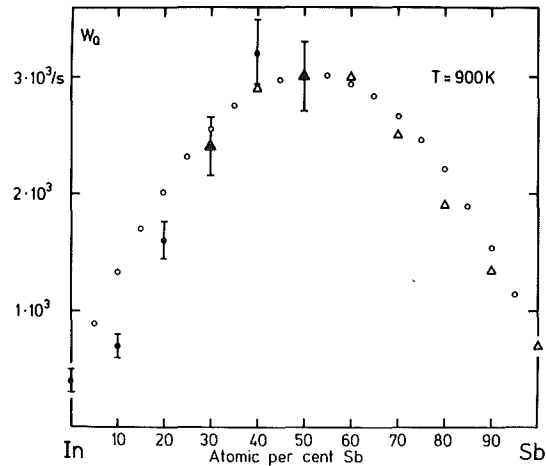
D. Quitmann, H. Hadijuana, W. v. Hartrott, J. Roßbach, E. Wehreter
Institut für Atom- und Festkörperphysik, Freie Universität Berlin

The perturbations of the nuclear spin orientation of a probe atom due to electric and magnetic fields in a solid or liquid surrounding depend sensitively on the electronic state and the arrangement and motion of the neighbouring atoms. These perturbations are usually measured by classical NMR as shifts and linewidths of the resonance signal, e.g. as a function of temperature or composition. They can also be measured by observing "in beam" the time differential angular distributions of the γ -radiation from nuclear isomers (ns ... ms range) which are produced and aligned by nuclear reactions. The method extends the possibilities of NMR in the sense that the effect (alignment) is independent of the matrix temperature; that one can observe quadrupolar interaction where no stable isotope with $I > 1/2$ exists; that isolated impurities are easy to study. We concentrate presently on spin relaxation measurements in the liquid state of semiconductor alloys because amorphous semiconductors have attracted considerable interest recently and the existing experimental material for hfi of this class of materials is scarce.

Essentials for the experiment are the following properties of the cyclotron: beams of p, d, α (hopefully Li) having high and sufficiently variable energy; focussing of the external beam on small targets (a few mm diameter); pulse structure of the beam with duty cycles $< 1:10$; rejection ratio of $< 10^{-4}$; pulse widths in the range 100 μ s ... 1 ns; average external beam current after pulsing 10 ... 100 nA. Here we mention two systems studied:

In_xSb_{1-x}: For these alloys we have measured relaxation rates W on ^{117m}Sb (340 μs) as a function of temperature T at fixed composition $x = 1$ and $x = 0.5$ and also as a function of composition ($0.3 < x < 1$) at fixed $T = 900^\circ \text{K}$. From these data together with existing NMR results on $^{121,123}\text{Sb}$; 1,2) $W_Q(\text{Sb InSb})$ is determined for the whole composition range, see the figure. This is of special interest as a test case for the theories of W_Q in liquid alloys and metals. The hump in W is due to an increase of the quadrupolar relaxation as expected for a substitutional alloy (statistical distribution of neighbouring ions carrying different charges according to their valency). From $W_Q(x = 0.5)$ we deduce the moment $|Q(^{117m}\text{Sb})| = 0.5 \text{ barn}$.

Fig. 1: W_Q of Sb in liquid
 In_x Sb_{1-x} alloys: Δ NMR data for ^{121}Sb ; \bullet TDPAD data for ^{117}Sb (normalized to Δ);
 \circ simplified theory for alloys 2)



In_xTe_{1-x}: This system shows behaviour typical for liquid metals ($x \approx 1$), liquid semiconductors ($x \approx 0.4$) and liquid semimetals ($x \approx 0$) ($T = 1000\text{K}$). We compare the hfi of ^{115}In (stable), ^{115m}Sn (160 μs) and ^{117m}Sb . At $x = 1$, the magnetic perturbation (if corrected for the nuclear moment and the multipolarity observed) is about the same at an In, Sn, or Sb probe atom. However, the quadrupolar perturbation (also corrected) increases in the ratio 3:20:65 from In to Sn to Sb, and this we ascribe to the increasing importance of the p-electrons. W_Q for ^{117m}Sb increases from $0.3 \cdot 10^3/\text{sec}$ to $50 \cdot 10^3/\text{sec}$ between pure In and In_2Te_3 , at 1000K. The alloying effect (see In-Sb) is strongly enhanced in this system, most probably due to charge transfer

from the metal to the Te atoms.

This work was supported by Deutsche Forschungsgemeinschaft through Sonderforschungsbereich 161.

References

- 1) W.W. Warren Jr. and W.G. Clark; Phys. Rev. 177 (1969) 600
- 2) E. Claridge et al. J.Phys. F2 (1972) 1162

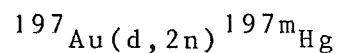
3.1.2 Hyperfine Interactions of ^{197}Au and $^{197\text{m}}\text{Hg}$ in Various Metals Studied by the Mössbauer Effect and Time-Differential Perturbed-Angular-Correlations

B. Perscheid, H. Büchsler, J.C. Soares, K. Freitag and M. Forker
Institut für Strahlen- und Kernphysik der Universität Bonn

An important method for the investigation of microscopic properties of metals is the study of the hyperfine interactions (HFI) at the site of dilute impurity ions in the impurity-metal-system. Among others such methods are the Mössbauer effect (ME) and the time-differential perturbed-angular-correlation (TDPAC), which both yield the interaction between the nuclear magnetic dipole and electric quadrupole moments of the impurity ion and the magnetic field and the electric field gradient at the site of the impurity.

In HFI studies on dilute impurities the sample preparation is one of the main problems. All impurity ions should occupy identical regular sites in an undamaged lattice. It is therefore of great importance to investigate the influence of the sample preparation on the experimental HFI parameters.

The Mössbauer nucleus ^{197}Au as dilute impurity is particularly favourable in this respect. The 77 keV Mössbauer transition is populated by the EC decay of ^{197}Hg . The ^{197}Hg activity can be produced by the reaction ¹⁾:



This reaction populates the 24 h - isomeric - $13/2^+$ -state of ^{197}Hg , which decays to the groundstate of ^{197}Hg via the 165 keV (M4) - 134 keV (E2) - cascade. This cascade is a well suited case for e^- - γ -TDPAC measurements ²⁾. The sources for the TDPAC and ME experiments have been prepared by ion implantation of $^{197\text{m}}\text{Hg}$ into metal foils by means of an electromagnetic mass-separator ³⁾. Then it is possible to study in the same source first the HFI of $^{197\text{m}}\text{Hg}$ by e^- - γ -TDPAC and after the decay of

^{197}Hg the HFI of ^{197}Au by ME. Furthermore one can check the influence of the source preparation on the HFI parameters by comparing the results of the implanted source with those obtained from a ME experiment using a source of ^{197}Pt molten with the host metal.

We have started a program to investigate the magnetic HFI in the 4f-ferromagnets Gd, Tb, Dy, Ho, Er and Tm and the electric HFI in the noncubic metal Be. In all studied cases we see that ion implantation does not yield the same results as melting. Especially the host metal Gd has been investigated very intensively with implanted sources of different impurity concentrations and various temperature treatments after implantation. But it was not possible to reproduce the results of the molten source ⁴⁾.

References

- 1) The deuteron irradiations were carried out at the Karlsruhe cyclotron
- 2) K. Krien et al. Phys. Rev. B8 (1973) 2248
- 3) The implantations were performed at the ISKP mass-separator
- 4) B. Perscheid et al., to be published

3.1.3 Mössbauer Spectroscopy with ^{61}Ni

G. Czjzek, J. Fink and H. Schmidt

Institut für Angewandte Kernphysik des Kernforschungszentrums Karlsruhe

Mössbauer spectroscopy has become a powerful tool for investigations in solid state physics and materials. Iron, cobalt and nickel are three of the most interesting elements in the first row transition metals, not only because of their widespread industrial applications, but also because of the richness of their magnetic properties. Two of these elements have isotopes which are well suited for Mössbauer spectroscopy: ^{57}Fe and ^{61}Ni . While most of the work in Mössbauer spectroscopy is done with ^{57}Fe , experiments with ^{61}Ni have not been as extensive for three reasons:

1. The half-life of a suitable ^{61}Ni source is short (1.6 h).
2. The production of a suitable ^{61}Ni source is difficult.
3. The shorter lifetime of the excited states results in a broader line width than that of ^{57}Fe , requiring spectra with small statistical errors for analysis.

In spite of these problems, we have started a program to investigate the electronic properties of transition metal alloys and compounds with ^{61}Ni Mössbauer spectroscopy.

The 67.4 keV state in ^{61}Ni can be populated by decay of the parent isotopes ^{61}Co and ^{61}Cu . ^{61}Cu is not suitable for source preparation because of the complexity of the decay scheme and because of the weak population of the 67.4 keV level. The reaction used was $^{64}\text{Ni}(p,\alpha)^{61}\text{Co}^{\beta^-} \rightarrow ^{61}\text{Ni}^*$ with a proton energy of about 18 MeV. This energy has been chosen to minimize the background in the γ -ray spectrum due to the 511 keV line caused by other reactions in the target. In order to get an unsplit emission line at 4.2 K, a nonmagnetic ^{64}Ni V (14 %) alloy has been produced and has been rolled to a foil approximately 0.15 mm thick. These targets have been cooled by circulating water during irradiation. The typical current has been 20 μA of H_2^+ ions and the irradiation time has been 40 min.

The Mössbauer spectra have been taken with a conventional Mössbauer spectrometer. For the detection of γ -rays a 3 mm NaJ(Tl)-detector has been used. Typical counting rates have been 250 000 counts/sec in the 67.4 keV line. In general, with one irradiation two Mössbauer spectra have been taken in a time of about 6 h.

During 1975, the main activity of ^{61}Ni Mössbauer spectroscopy work was devoted to the investigation of the Mott insulator NiS_2 and the metalinsulator transitions induced by the introduction of vacancies and copper impurities into NiS_2 and by the replacement of S by Se. The work was done in collaboration with the Laboratoire de Structure Electronique des Solides of the University of Strasbourg. In pure NiS_2 , measurements of the hyperfine coupling constants at the ^{61}Ni nuclei revealed important information on the unknown magnetic structures of this compound. The introduction of vacancies on the nickel sublattice leads to a substantial change of the electrical resistivity which approaches metallic behaviour near 5 % vacancies. The results of the ^{61}Ni Mössbauer experiments are interpreted on the basis of local electronic states associated with vacancies. An increase of the vacancy content leads to an overlap of the regions of the local electronic states, thus giving metallic conductivity. The changes of the properties observed upon introduction of copper impurities are qualitatively similar to those in materials containing nickel vacancies. The investigation of the mixed compound $\text{NiS}_{2-x}\text{Se}_x$ by ^{61}Ni Mössbauer spectroscopy showed the occurrence of an anti-ferromagnetic metallic phase for $0.47 \leq x \leq 1.0$. This phase had been predicted in connection with a metal-insulator transition by Mott, Cyrot and others, but it had not been found until now. In addition, a significant change of the magnetic structure with replacement of S by Se was observed.

Furthermore, the magnetic properties of disordered Ni-Mn alloys were investigated by ^{61}Ni Mössbauer spectroscopy during 1975. The interest in this alloy system is based on the unusual magnetic properties associated with the transition from ferromagnetic for Ni-rich alloys to an antiferromagnetic ordering of alloys

with Mn concentrations greater than about 30 at. %. The concentration dependence of the total average of the magnetic hyperfine fields at the ^{61}Ni nuclei is very similar to that of the bulk magnetization for $C_{\text{Mn}} \leq 0.2$. For higher Mn concentrations, the bulk magnetization drops rapidly upon further addition of Mn and vanishes for $C_{\text{Mn}} \sim 0.28$, whereas the magnetic hyperfine fields are remarkably constant, showing a continuous transition from ferromagnetism to antiferromagnetism. The character of the distribution of magnetic hyperfine fields indicates the occurrence of magnetic clusters in this concentration range. Studies of the alloy systems Dy-Ni-Fe and Pd-Ni-Fe and of amorphous NiP alloys have been started.

3.1.4 The Hyperfine Field of Mercury in Iron*

K. Freitag and P. Herzog, Institut für Strahlen- und Kernphysik der Universität Bonn and

P.K. James and N.J. Stone, Mullard Cryomagnetic Laboratory, Clarendon Laboratory, Oxford

Recently the magnetic hyperfine field of mercury in an iron host has been studied extensively. Several techniques and isotopes have been used for these investigations. The methods which seem to give the most reliable results were time differential perturbed angular correlations (TDPAC) measured at room temperature and nuclear magnetic resonance on oriented nuclei (NMR/ON) performed at temperatures below 1K with the isotope ^{203}Hg . Whereas the TDPAC experiments gave a field slightly under 700 kG, the NMR/ON result was 838 kG. To further investigate this discrepancy we performed an NMR/ON experiment on the isotope $^{197\text{m}}\text{Hg}$, the same isotope which had been used for some of the TDPAC experiments.

The 24 hours activity $^{197\text{m}}\text{Hg}$ was produced by deuteron irradiation of gold in the Karlsruhe cyclotron. It was subsequently implanted into iron with the Bonn mass separator. The NMR/ON experiment was performed in a paramagnetic demagnetisation apparatus in Oxford. The anisotropy destruction of the 134 keV γ -radiation from the decay of oriented $^{197\text{m}}\text{Hg}$ nuclei was studied in dependence of the applied radio frequency. In fig. 1 the percentage destruction of anisotropy is shown as obtained a) for increasing, b) for decreasing frequency. The dotted curve represents the intrinsic lineshape of the resonance; the solid lines are the fitted curves taking into account relaxation. From the centre frequency of 101.18(10) MHz $B_{\text{hf}}(\text{HgFe}) = 839.5(8)$ kG is derived using $\mu = 1.027684(3)$ for the magnetic moment of $^{197\text{m}}\text{Hg}$. This value is in good agreement with the result of the NMR/ON experiment on ^{203}Hg . Thus we are led to the conclusion that the difference between the TDPAC results at room temperature and the NMR/ON results below 1K must be ascribed to an anomaly in the temperature dependence of the field of mercury in iron. Further TDPAC experiments at intermediate temperatures should be undertaken to confirm this hypothesis.

*) Details and references can be found in a paper by the same authors to be published in Phys. Rev. B, early 1976

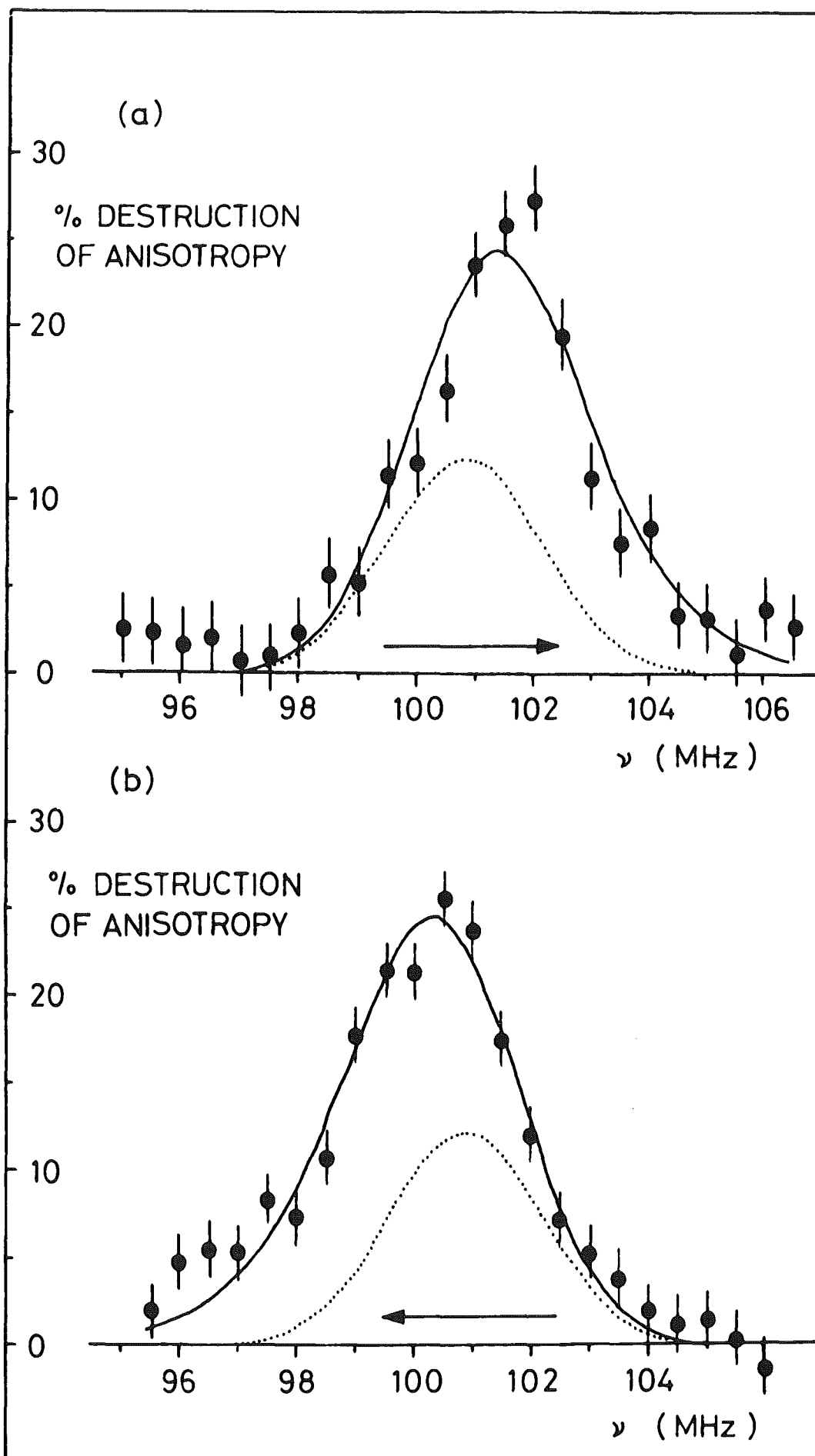


Fig. 1: The anisotropy destruction of the 134 keV γ -radiation from the decay of oriented ^{197m}Hg nuclei in an iron host

3.2 Engineering

3.2.1 Thin Layer Radioactivation of Machine Components

G. Essig, E. Rühl

Laboratorium für Isotopentechnik des Kernforschungszentrums Karlsruhe

In the field of wear measurements on machine components radio-nuclide methods have been gaining increased importance. This development was spurred by the introduction of thin layer radio-activation with charged particles. This new technique made it possible to create a thin layer of high specific activity on the surface of components independent of their weight.

This active surface layer of a few hundred micrometers thickness allows most sensitive measurements with total activities of several hundred microcuries only.

In 1975 the irradiation group of the Laboratorium für Isotopentechnik, Abteilung Physik/Maschinenbau, used the cyclotron for about 900 hours or 15 % of operating time.

A hundred hours were dedicated to experimental radioactivation. During irradiations for wear measurements several concurrent nuclear reactions usually take place, because the materials used normally consist of a mixture of elements and isotopes (metal alloys, natural isotope mixtures). The general formula for any such reaction can be written as

$$K_i(a, b_j)K_R^+ \quad \text{with } a: p \text{ or } d \text{ or } \alpha$$
$$b_j: n, 2n, 3n$$
$$p$$
$$\alpha$$
$$t$$

For any given target nuclide K_i an energy interval is determined for which the compound cross sections for all concurrent reactions with the product K_k^+ has its maximum. The most suitable K_k^+ is determined by the measurement task at hand. Typical parameters are materials, half life, gamma energies, and yield. The cross sections are derived from either irradiations of foil packages or measurements of the activity of irradiated thick targets which are

gradually ground off. For most alloys the second method has to be used because suitable foils are not available.

800 hours of cyclotron time were used to irradiate 120 machine components for wear measurements. One third of this time was necessary for activations for industry or research laboratories outside the Laboratorium für Isotopentechnik, Abteilung Physik/Maschinenbau, equipped with their own RNT measuring units. Most targets weighed 5 to 150 Newton, their activities were some hundred microcuries.

For most irradiations the target has to be moved in front of the fixed particle beam by a programmable irradiation facility in order to get an evenly distributed activity of the wear zone. This facility is shown on the photograph. The extraction head of the beam tube can be seen on the left. In front of it a cylinder head is mounted on the irradiation facility. It was rotated for an activation of a ring zone on a valve seat.

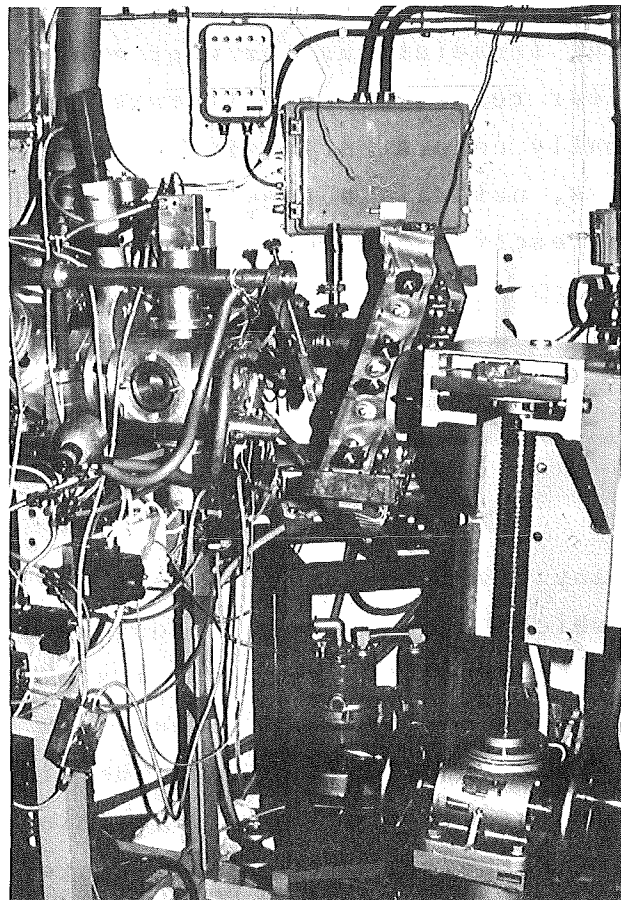


Fig.1: Activation of a valve seat on a machined cylinder head for an automobile engine

3.2.2 Use of Cyclotron Activated Fluorine-18 in Investigations Relating to Process Engineering

J. Schmitz, A. Merz, Laboratorium für Isotopentechnik des Kernforschungszentrums Karlsruhe

The Laboratory of Isotope Techniques (LIT) together with Kali-Chemie AG have performed a test program with the aim of defining technical process parameters in the Rhenania fertilizer production carried out in rotary kilns. The technical characteristics so determined are to form the basis for optimum processing and to give indications for plant construction.

One of the test series performed at the rotary kiln are related to the study of problems connected with fluorine. Although fluorine contamination present as apatite in the crude phosphate leaves the furnace mainly together with klinker, there was no knowledge of a possible fluorine circulation and enrichment in the furnace holdup and of a transition into the process dust or into the waste gas.

A test performed with NaF (Na-24 labelled) did not provide information regarding fluorine. To elucidate the questions unsettled only direct tracing of apatite by F-18 was meaningful. Therefore, F-18 labelled CaF_2 was added to the feed stream and its behavior in the kiln was surveyed by scintillation detectors placed outside the reactor, at the cyclones and in the waste gas stream. CaF_2 labeling with high specific activity was possible only at a powerful cyclotron, e.g., in the Federal Republic of Germany only Karlsruhe, using fast (20 MeV) neutrons (n,2n reaction). For this purpose, CaF_2 pellets were subjected to test irradiations at the cyclotron, first in the external proton beam and later-on in the internal beam because of the higher current intensity achievable, so that the activity distribution in the given sample geometry and the maximum attainable F-18 activity could be determined.

Behind the water-cooled Be-target the CaF_2 pellets (\emptyset 18 mm) were arranged in a cylindric geometry in a sealed ampoule made of high-purity quartz. The diagram shows the specific F-18 activity determined, normalized with the current integral, as a function

of the sample length. With the current intensity available of 35 μA and a irradiation time of about 2 half lives some 150 mCi F-18 were obtained with the given sample size at the end of irradiation.

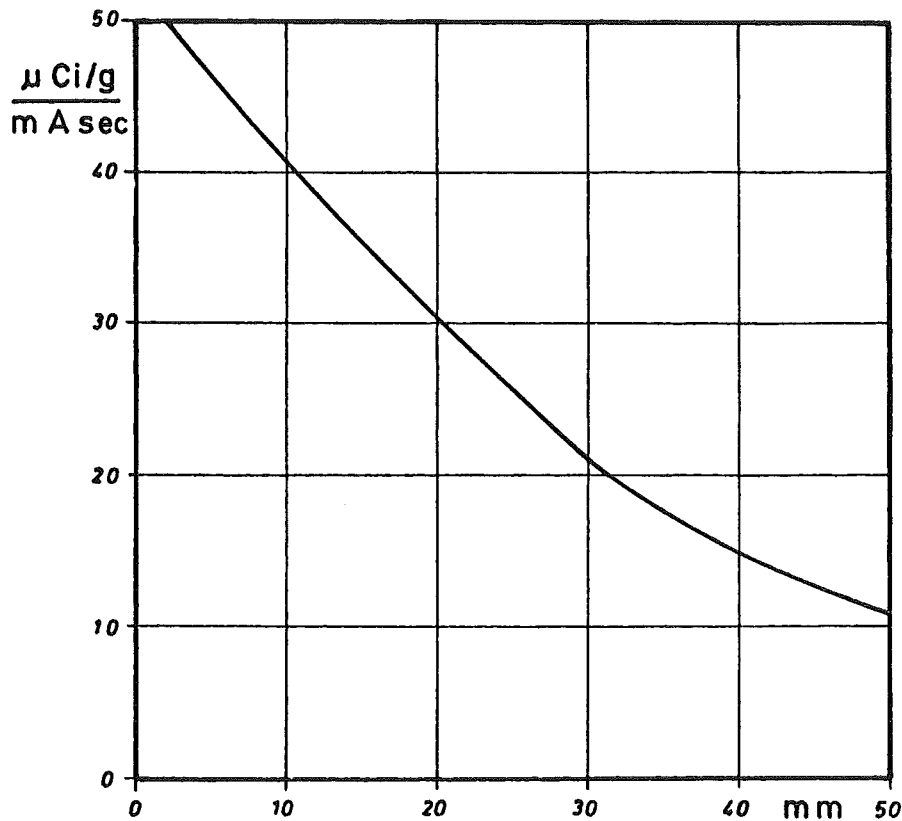


Fig. 1: Specific F-18 activity related to the current integral as a function of the sample length

Due to the short half life (110 min) transportation from Karlsruhe to the 700 km distant testsite had to be done by airplane. Only this way the 40 mCi minimum activity necessary for the experiment could be introduced into the rotary kiln already 3.5 hours after the irradiation.

This test showed that the mechanism of movement of CaF_2 in the rotary kiln did not differ from the other reactants. No activity was found in the process dust. However, fluorine appeared periodically in the waste gas, especially when the labelled mass passed the chemical reaction zone.

3.3 Nuclear Medicine

3.3.1 The Production of Radionuclides ^{123}I , ^{77}Br for Nuclear Medicine with High Energetic ^4He Particles

F. Helus, W. Maier-Borst, Deutsches Krebsforschungszentrum, Institut für Nuklearmedizin, Heidelberg

R.M. Lambrecht, A.P. Wolf, Brookhaven National Laboratory, Chemistry Department, Upton, New York 11973, USA

Introduction

The desirable physical characteristics of iodine-123 that make the nuclide, if used in high radionuclidic purity, nearly ideal for radiopharmaceutical applications are well known. The highest purity ^{123}I available is produced from the $^{123}\text{Xe} \xrightarrow{2.1\text{hr}} ^{123}\text{I}$ generator, since the radiohalogens produced by direct nuclear reactions can be removed from ^{123}Xe parent before it decays to ^{123}I (1,11). The radioiodine of consequence is then ^{125}I , which arises from the concurrent production of ^{125}Xe with ^{123}Xe and the decay of ^{123}Xe ($^{125}\text{Xe} \xrightarrow{16.8\text{hr}} ^{125}\text{I}$) simultaneously with the decay of the ^{123}Xe . A compilation of some literature described reactions for direct production of iodine-123 is listed in Table 1.

Reaction	Incident beam energy (MeV)	Target material (natural enriched %)	Thick target yield (mCi/ μAh)	References
$^{121}\text{Sb}(^4\text{He}, 2n)^{123}\text{I}$	25	Sb - nat.	0.150	(2)
$^{123}\text{Sb}(^3\text{He}, 3n)^{123}\text{I}$	23	Sb - nat.	0.024	(3)
$^{122}\text{Te}(d, n)^{123}\text{I}$	7	Te - 95.4	0.100	(1)
$^{123}\text{Te}(p, n)^{123}\text{I}$	19	Te - 79.0	0.440	(1)
$^{124}\text{Te}(p, 2n)^{123}\text{I}$	28	Te - 91.9	24.3	(16)
$^{125}\text{Te}(p, 3n)^{123}\text{I}$	36	Te - 95.5	0.85	(1)

Tab. 1: Reported methods of ^{123}I production - Direct reactions

Most of the cyclotron production methods producing ^{123}Xe have been evaluated and are shown in Table 2.

Reaction	Incident beam energy (MeV)	Target material (natural enriched %)	Thick target yield (mCi/ μAh)	Reference
$^{122}\text{Te}(\alpha, 3n)^{123}\text{Xe}$	46	Te - 95.0	0.200	(4)
$^{122}\text{Te}(^3\text{He}, 2n)^{123}\text{Xe}$	27	Te - 90.0	0.530	(1)
$^{123}\text{Te}(^3\text{He}, 3n)^{123}\text{Xe}$	30	Te - 76.5	1.10	(1)
$^{127}\text{I}(p, 5n)^{123}\text{Xe}$	57.5	I_2 - nat.	3.0	(5)
$^{127}\text{I}(d, 6n)^{123}\text{Xe}$	78	NaI - nat.	8.0	(6)
$^{124}\text{Te}(\alpha, 5n)^{123}\text{Xe}$	85	Te - nat.	0.250	(7)
$^{127}\text{I}(\alpha, 8n)^{127}\text{Cs}$	102	NaI - nat.	-	this work

Tab 2: Reported methods of ^{123}I production. Generator system $^{123}\text{Xe} \xrightarrow{\beta^+, \text{EC}} ^{123}\text{I}$

The alpha reaction with 46 MeV alpha's has been in routine production ⁴⁾ as a source of ^{123}I for clinical use. The proton ⁵⁾ and deuteron ⁶⁾ spallation reactions $^{123}\text{J}(p, 5n)^{123}\text{Xe}$, $E_H=50-60$ MeV and $^{127}\text{I}(d, 6n)^{123}\text{Xe}$, $E_D=65-69$ MeV result in ^{123}I of nearly comparable purity. Certain accelerators such as Karlsruhe cyclotron have 102 MeV alphas, but protons and deuterons too low energy to produce ^{123}Xe by either reaction.

In this study we have tested the feasibility of using high energy alpha reactions to produce $^{123}\text{Xe} \rightarrow ^{123}\text{I}$ generator. Alpha reactions on ^{127}I (100 % natural abundance) were tested. The reactions concerned are shown in Table 3. Nuclear reactions with high energy particles are more complicated than lower energy reactions. From our preliminary experiments it followed that ^{123}I is produced in two different ways - either by the direct reaction or indirectly via ^{123}Cs or ^{123}Xe . When we consider only very simple reaction mechanism then last two reactions in Table 3 described directly produced ^{123}I . For indirectly produced ^{123}I we assume the reactions $^{127}\text{I}(^4\text{He}, 8n)^{123}\text{Cs}$ and $^{127}\text{I}(^4\text{He}, p7n)^{123}\text{Xe}$.

Reaction	Q (MeV)
$^{127}\text{I}(^4\text{He},4\text{n})^{127}\text{Cs} \rightarrow ^{127}\text{Xe} \rightarrow ^{127}\text{I} \text{ (stab.)}$	-32.61
$^{127}\text{I}(^4\text{He},5\text{n})^{126}\text{Cs} \rightarrow ^{126}\text{Xe} \text{ (stab.)}$	-42.75
$^{127}\text{I}(^4\text{He},6\text{n})^{125}\text{Cs} \rightarrow ^{125}\text{Xe} \rightarrow ^{125}\text{I}$	-50.91
$^{127}\text{I}(^4\text{He},7\text{n})^{124}\text{Cs} \rightarrow ^{124}\text{Xe} \text{ (stab.)}$	-61.50
$^{127}\text{I}(^4\text{He},8\text{n})^{123}\text{Cs} \rightarrow ^{123}\text{Xe} \rightarrow ^{123}\text{I}$	-70.04
$^{127}\text{I}(^4\text{He},^4\text{He} \text{ n})$	- 9.14
$^{127}\text{I}(^4\text{He},^4\text{He}2\text{n})^{125}$	-16.24
$^{127}\text{I}(^4\text{He},^4\text{He}3\text{n})^{124}\text{I}$	-25.84
$^{127}\text{I}(^4\text{He},^4\text{He}4\text{n})^{123}\text{I}$	-33.30
$^{127}\text{I}(^4\text{He},2\text{p}6\text{n})^{123}\text{I}$	-61.10

Table 3

Reactions $(\alpha,8\text{n})$ and $(\alpha,6\text{n})$ have been studied previously ¹²⁾, but the objective of that study was the identification and nuclear decay properties of ^{123}Cs and ^{125}Cs . Cross-section and yield data have not been reported. Xenon was separated from the target material by using two different techniques - generator method of Sodd ¹⁾ and chemical method.

Bromine-77 appears to be the best bromine nuclide, because it has a 56 hr half-life and lower energy gamma radiation than either ^{76}Br or ^{82}Br . The published production methods and potential production reactions are shown in Table 4.

Direct reaction	Q (MeV)	Reference
$^{75}\text{As}(^4\text{He},2\text{n})^{77}\text{Br}$	-13.51	(9)
$^{76}\text{Se}(\text{d},\text{n})^{77}\text{Br}$	- 3.04	-
$^{78}\text{Se}(\text{p},2\text{n})^{77}\text{Br}$	-12.64	-
Indirect reaction		
$^{76}\text{Se}(^4\text{He},3\text{n})^{77}\text{Kr} \rightarrow ^{77}\text{Br}$	-26.81	(10)
$^{76}\text{Se}(^3\text{He},2\text{n})^{77}\text{Kr} \rightarrow ^{77}\text{Br}$	- 6.23	-
$^{79}\text{Br}(\text{p},3\text{n})^{77}\text{Kr} \rightarrow ^{77}\text{Br}$	-22.76	-
$^{79}\text{Br}(^4\text{He},6\text{n})^{77}\text{Rb} \rightarrow ^{77}\text{Kr} \rightarrow ^{77}\text{Br}$	-48.44	this work

Table 4: Methods of ^{77}Br production

Production of ^{77}Br by the alpha particle bombardment of arsenic pentoxide has been made on routine basis for clinical use ^{9,13}). In future ^{77}Br may find use in generator systems ¹⁰) as a label for bromine compounds and as an alternative to iodine when preparing radiopharmaceuticals ¹⁴). Advantage in producing ^{77}Br by means of ^{77}Kr decay is the possibility of excitation labeling. In the production method described here, natural sodium bromide is bombarded with alpha particles in the energy range 50-102 MeV.

Experimental

The irradiations were performed at the Kernforschungszentrum cyclotron at Karlsruhe ¹⁵). Energy selection was made by placing the internal target at the appropriate radius in the cyclotron. The integrated dose was measured only by the integration of the cyclotron beam current. For the yield figures the irradiation dose was 150 μAsec at a beam current of 0.6 μA . The salt targets were pressed at 10 kp/cm^2 and mounted in an Al target holder (5 mm x 7 mm x 11 mm) and sealed with a 0.020 mm Al foil of 99.99% purity. The thickness of sodium iodide and bromide (Merck) salt targets varied from 150 to 160 mg/cm^2 . Identification and assay of gamma ray emitting radionuclides were done on a 4096-channel Ge(Li) Intertechnique spectrometer combined with a Multi-20 small computer. The computer provided photopeak integration, a spectral plot and half-life information. Because of the transportation distance between Karlsruhe and Heidelberg, it was not possible to assay radionuclides with very short half-lives.

The thick target yield of radionuclides produced by 100 MeV alpha bombardment of sodium iodide were determined and are listed in Table 5.

^{124}I and ^{126}I nuclides can be produced only by direct reactions, because ^{124}Xe and ^{126}Xe are stable isotopes. The most probable reactions to produce ^{124}I and ^{126}I directly are shown in Tab. 3. Presence of all directly produced radionuclides does not affect the radionuclidic purity of the ^{123}I if the radioxenons are separated from the NaI either during or immediately after the irradiation.

Nuclide	Half-life	E (keV)	Analyzed gamma-lines abundance %	Thick target yield $\mu\text{Ci}/\mu\text{Ah}$ EOB
^{121}I	2.12 h	212,50	84.3	1359.4
^{121}Te	17.00 d	573.08	79.1	5.6
^{123}Xe	2.08 h	148.70	50.0	541.6
^{123}I	13.30 h	159.10	83.0	684.0
^{124}I	4.17 d	602.71	62.0	34.2
^{125}Xe	16.80 h	188.43	55.0	1022.9
^{125}I	60.14 d	calculated from ^{125}Xe		12.1
^{126}I	12.80 d	388.47	35.4	24.9
^{127}Cs	6.25 h	411.10	63.0	1812.9
^{127}Xe	36.41 d	202.84	58.2	22.0

Table 5: Radionuclides produced by 100 MeV alpha bombardment of sodium iodide

Table 6 summarizes the thick target yield measurements for the production of ^{123}Xe by bombardment of NaI with 60-102 MeV alphas.

E_{α} MeV	Thick target yield of ^{123}I		
	Direct produced $\mu\text{Ci}/\mu\text{Ah}$ ^{123}I	Indirect produced $\mu\text{Ci}/\mu\text{Ah}$ ^{123}Xe $\mu\text{Ci}/\mu\text{Ah}$ ^{123}I	
60	9.0	-	-
70	84.8	-	-
80	204.1	-	-
85	254.2	11.4	3.1
90	328.4	65.2	17.4
95	415.2	225.2	60.1
100	539.3	541.6	144.7
102	526.9	626.8	167.1

Table 6: Production rates of direct and indirect ^{123}I produced by 60-102 MeV alpha bombardment of sodium iodide

The data indicate that the production rate of ^{123}Xe increases from 11.4 to 626.8 $\mu\text{Ci}/\mu\text{Ah}$ between 85 and 102 MeV. ^{123}Xe was not observed at $E_\alpha < 85$ MeV.

The yield of ^{123}Xe and its corresponding yield of ^{123}I is too low, and the production rate of ^{125}I too high (as follows from Table 4), to make the alpha reactions on ^{127}I of practical value at these energies.

Similar work has been done to investigate the possibility to produce $^{77}\text{Kr} \rightarrow ^{77}\text{Br}$ generator. The production rates obtained for directly and indirectly produced ^{77}Br with 60-102 MeV alphas are given in Table 7.

E_α MeV	Thick target yield of ^{77}Br		
	Direct produced $\mu\text{Ci}/\mu\text{Ah}$ ^{77}Br	Indirect produced $\mu\text{Ci}/\mu\text{Ah}$ ^{77}Kr	Indirect produced $\mu\text{Ci}/\mu\text{Ah}$ ^{77}Br
60	30.50	-	-
65	53.90	-	-
70	76.46	34.20	0.77
75	89.21	87.52	1.98
80	81.87	254.14	5.75
85	123.53	513.72	11.63
90	172.90	621.20	14.13
95	238.25	1298.30	29.40
100	281.28	1784.50	40.41

Table 7: Production rates of direct and indirect ^{77}Br produced by 50-102 MeV alpha bombardment of sodium bromide

^{77}Kr yield increases very rapidly from 34 to 1784 $\mu\text{Ci}/\mu\text{Ah}$ with alpha energy from 70 to 102 MeV. From yield figures at 100 MeV alpha energy it follows that only about 12 % of the obtained ^{77}Br is produced via ^{77}Kr . The nuclear reactions leading to ^{77}Br and ^{77}Kr are expected to occur more favorably for routine production of ^{77}Br only when higher beam currents or higher alpha energy are available.

Table 8 summarizes production rates of radionuclides produced by 100 MeV alphas.

Nuclide	Half-life	Analyzed gamma-lines		Thick target yield ($\mu\text{Ci}/\mu\text{Ah EOB}$)
		E_{γ} (keV)	abundance %	
^{75}As	17.7 d	595.7	59.5	2.32
^{75}As	120.0 d	135.9	58.0	3.74
^{75}Br	100.0 m	286.5	80.0	748.56
^{76}Br	15.0 h	559.0	65.7	380.40
^{77}Kr	1.24 h	129.7	84.0	1784.50
^{77}Br	56.7 h	238.9	26.0	321.70
^{79}Kr	34.9 h	261.3	11.0	265.13
^{81}Rb	4.7 h	446.3	23.5	1631.06
$^{82\text{m}}\text{Rb}$	6.4 h	776.8	83.0	236.77
^{83}Rb	83.0	529.6	30.4	2.66

Table 8: Radionuclides produced by 100 MeV alpha bombardment of sodium bromide

The most important impurity is ^{76}Br from the decay of ^{76}Kr . This can be limited by allowing the ^{77}Kr to decay only for three half-lives. By using the gas flow system ^{77}Kr can be separated from directly produced radiobromines and other contaminants. This is the first report of the use of 70-120 MeV alpha bombardment to produce $^{77}\text{Kr} \rightarrow ^{77}\text{Br}$ generator.

References

1. V.J. Sodd, J.W. Blue and H.N. Wellmann; U.S. Department of Health, Education and Welfare Publication BRH/DMRE 70-4 (1970)
2. D.J. Silvester, J. Sugden and I. Watson; Radiochem. Radioanal. Letters 2 (1969) 17
3. J.R. Dahl and R.S. Tilbury; Int. J. Appl. Rad. Isotopes 23 (1972) 431
4. R.M. Lambrecht, A.P. Wolf; Radiation Research 52 (1972) 32
5. M.A. Fusco, et al.; J. Nucl. Med. 13 (1972) 729
6. R. Weinreich, O. Schult and G. Stöcklin; Int. J. Appl. Rad. Isotopes 25 (1974) 535
7. R.M. Lambrecht, et al.; (in press)
8. G. Erdtmann, W. Soyka; Die α -Linien der Radionuklide, KFA Jül-1003-AC, Apr. 1974
9. F. Helus; Radiochem. Radioanal. Letters 3 (1970) 45
10. J.W. Blue and P.P. Benjamin; J. Nucl. Med. 12 (1971) 416
11. R.M. Lambrecht; J. Nucl. Med. 13 (1972) 266
12. H.B. Mathur and E.K. Hyde; Phys. Rev. 96 (1954) 126
13. A.D. Nunn; Nucl. Instruments and Methods 99 (1972)
14. T. Sargent, et al.; J. Nucl. Med. 16 (1975) 243
15. F. Schulz and H. Bellemann; KFK-Report 685 (1967) Karlsruhe
16. E. Acerbi, et al.; 11th European Cyclotron Progress Meeting, Louvain, June 1974

3.3.2 Studies of Chemistry and Potential Nuclear Medical Application of ^{211}At

K. Rössler, G.-J. Meyer and G. Stöcklin

Institut für Chemie der Kernforschungsanlage Jülich GmbH

Institut 1: Nuklearchemie

The radioelement astatine, the heavier homologue of iodine, and especially its α -emitting, short-lived isotope ^{211}At ($T=7.2$ h) is of potential interest for radiation biological and therapeutical applications. It might be used as an internal radiation source for α -therapy, provided it can be administered in a suited chemical form for selective incorporation into specific organs or centres of disease. The chemistry of astatine, due to its unusual oxidation potentials and the increased metallic character of this halogen, is somewhat different than that of iodine. Thus, a study of its reactivity is a necessary condition for a successful labelling of biomolecules. Especially, DNA-precursors are of great interest, since these substances might serve as a vehicle for ^{211}At to the nuclei of heavily proliferating cells, e.g. in tumors, cf. (1).

The astatine was produced via the $^{209}\text{Bi}(\alpha, 2n)^{211}\text{At}$ nuclear process by 30 MeV α 's. Its separation and transfer to simple inorganic forms was achieved by both, wet dissolution and distillation as well as dry distillation procedures ^{1,2)}. With respect to the labelling of biomolecules we studied the mechanism of the reactions of At^- , At^0 , At^+ , AtCl , AtBr with benzene derivatives (halobenzenes, toluene, aniline) and pyrimidine-bases (Uracil (U) and deoxyuridine (UdR)) with the aid of radiogas- and high pressure liquid chromatography ³⁻⁵⁾.

Using AtCl and IUdR as reactants $^{211}\text{AtUdR}$ yields ranging from 5 to 10 % were obtained. A more selective labelling and higher yields (up to 30 %) could be reached by the decomposition of the corresponding 5-diazonium salts in the presence of At^- . To test this type of reaction, we applied it to the preparation

of the ortho-, meta- and para-isomers of astatofluoro-, astatochloro-, astatobromo- and astatiodobenzenes ⁴⁾. Most of these compounds were prepared for the first time. Starting from 5-aminouracil and 5-aminodeoxyuridine we achieved the synthesis of 5-At-U and 5-AtUdR ^{3,5)}.

Studies of the distribution and metabolism of inorganic astatine species as well as labelled biomolecules in healthy mice and those bearing an experimental tumor (Sarkoma 180) revealed a certain enrichment in the tumors and those organs containing a large amount of reticuloendothelial cells ^{3,6)}. This can be attributed to the phagocytosis by macrophages.

References

1. K. Rössler, W. Tornau and G. Stöcklin; J. Radioanalyt. Chem. 21 (1974) 199
2. G.-J. Meyer; Report-Jül-1076-NC (1974)
3. G.-J. Meyer, K. Rössler and G. Stöcklin; AED-CONF-75-404-029 (1975)
4. G.-J. Meyer, K. Rössler and G. Stöcklin; Radiochem. Radioanalyt. Letters 21 (1975) 247
5. G.-J. Meyer, K. Rössler and G. Stöcklin; J. Lab. Comp. Radiopharm., in press
6. M. Persigehl and K. Rössler; AED-CONF-75-193-078 (1975)

3.3.3 Investigation of the Suitability of ^{125}Xe for Application in Nuclear Medicine

S. Göring, A. Hanser, G. Haushahn, G. Schatz, Institut für Angewandte Kernphysik des Kernforschungszentrums Karlsruhe
W.E. Adam, F. Bitter, H. Kampmann, Department für Radiologie der Universität Ulm

In nuclear medicine radioactive ^{133}Xe is currently used to examine pulmonary function and blood flow. However, the relatively low gamma ray energy of ^{133}Xe (81 keV) is less suited for recording scintigrams, since the resolution of scinticameras is approximately inversely proportional to the square root of gamma ray energy. A substantial improvement is expected from the substitution of ^{133}Xe by ^{125}Xe which emits gamma quanta of 188 keV (frequency 55 %) and 243 keV (frequency 29 %) ¹⁾. ^{125}Xe can be produced sufficiently pure in an accelerator only. Considerations and preliminary tests have shown that it should be possible to procedure 250 mCi/h ^{125}Xe at the Karlsruhe Cyclotron according to the following scheme: Irradiation with 45 MeV deuterons of a circulating concentrated NaI solution in the internal cyclotron beam with about 50 μA beam current; continuous separation of the radioactive xenon formed by means of a helium gas flow passing through the target liquid at an appropriate point of its circulating path and from which xenon can be separated again by freezing out. To test the improvement of the quality of scintigrams when ^{125}Xe is used instead of ^{133}Xe , linear sources, i.e. little glass tubes of 2 mm diameter, containing ^{125}Xe and ^{133}Xe , respectively, were reproduced with a scinticamera of Ulm University, providing a 10 cm distance between the source and the collimator of the camera. In a second measurement the space between the source and the collimator was filled with paraffin to simulate the influence of scattering tissue between the body organ to be pictured and the camera. The table contains the resolutions (FWHM) so obtained. In the last column of the table values are given as a comparison, which have been calculated according to the formula

$$R_{\text{calc.}} = \sqrt{R_i^2 \cdot \frac{140}{E_\gamma} + R_{\text{coll.}}^2}$$

where

R_i = resolution of the camera for 140 keV gamma energy;
it is 10 mm according to the manufacturer;

E_γ = gamma energy in keV used for picturing;

$R_{\text{coll.}}$ = collimator resolution in mm at 10 cm distance ²⁾.

These values are applicable for recording without paraffin absorber.

The relatively little improvement achieved by the use of ¹²⁵Xe renders a bit doubtful whether this advantage will make up for the drawback of ¹²⁵Xe characterized by a less practicable half-life of only 17 h and higher production costs (¹³³Xe can be produced in the reactor).

Nuclide	Gamma Energy keV	Resolution (FWHM) in mm		$R_{\text{calc.}}$
		measured without paraffin	with absorber	
¹³³ Xe	81	21.2	22.8	18.8
¹²⁵ Xe	189	18.5	20.0	15.9
	243	18.4	20.1	15.4

Table 1

References

1. E.g. N.S. McDonald; AED-Conf. 74-020-027
2. J. Tolwinski, B.A. Gwiazdowska, H. Mackiewicz;
Nuklearmedizin 12 (1974) 346

3.3.4 Potassium-43 Production

F. Michel, H. Münzel, Institut für Radiochemie des Kernforschungszentrums
Karlsruhe

Radioactive isotopes of potassium are used for a number of applications in medical diagnostics, such as heart examination. The reader is referred to Clark et al. ¹⁾ for a compilation of literature. Mainly ^{42}K was used in the investigations because it can be conveniently produced by reactor irradiations. However, this nuclide is not well suited for γ -scintography on account of the very high energy of γ -radiation. Due to the low absolute abundance of γ -radiation high activities must be administered to the patients. By its decay data ^{43}K is much better suited for diagnosis.

The $^{40}\text{Ar}(\alpha, p)^{43}\text{K}$ reaction is best suited for routine ^{43}K production. The activity formed in the argon irradiation is almost uniformly distributed over the walls of the relatively large target chamber and must be washed off to allow subsequent treatment. Undoubtedly, this entails considerable difficulties in routine production. Therefore, Clark et al. ¹⁾ developed a method according to which argon is permanently circulated by a pump and the potassium formed filtered continuously. The yield is 70 to 80 % according to the authors. However, according to the experience gained with helium jet systems the yield must be expected to vary considerably. Another drawback of this method is that the diaphragm pumps are installed in the hot zone and must work permanently during irradiation. These difficulties could be avoided by electrostatic collection of the reaction products on an electrode. Already in 1959 Dyson and Francois ²⁾ attempted to employ this principle in the production of ^{43}K . However, the results obtained were little satisfactory. The yield was only about 30 %. Moreover, irradiation and collection alternated so that only about 50 % of the irradiation time was effectively used for nuclide production. As a matter of fact, the publication by Dyson and Francois left quite a number of questions open so that it seemed reasonable to reexamine the results.

In the investigations argon was irradiated in a target chamber consisting of a glass tube (30 cm in length, 5 cm in diameter), the leading end of which had been sealed by a flange provided with a beam window (diameter 2 cm; cover made of Havar foil). The potassium activities formed were either collected on an aluminium foil or on a stainless steel tube (diameter 4 mm) by applying a voltage of 500 to 2000 V. The energy of the projectile was varied by a relatively thick graphite disk and thin aluminium foils. Both the influence of the voltage applied and of the projectile energy on the ^{43}K yield were investigated. The results obtained can be summarized as follows:

- The yields published by Clark et al.¹⁾ have been largely confirmed. However, higher yields were obtained with low projectile energies, which is due to the larger spread in the projectile energy resulting from deceleration.
- Roughly 90 % of the ^{43}K activity formed are deposited on the stainless steel tube. The rest of activity can be found on the opposite electrode.

It was consequently shown that the potassium formed in a gas target can be deposited electrostatically with a high yield on an electrode conveniently shaped for routine production. This method is also applicable in the production of carrierfree rubidium isotopes by irradiation of krypton with protons or deuterons. By contrast, ^{18}F formed during irradiation of oxygen is neither preferably deposited on the anode nor on the cathode. A detailed description of the results of the investigation will be published shortly as an external report³⁾.

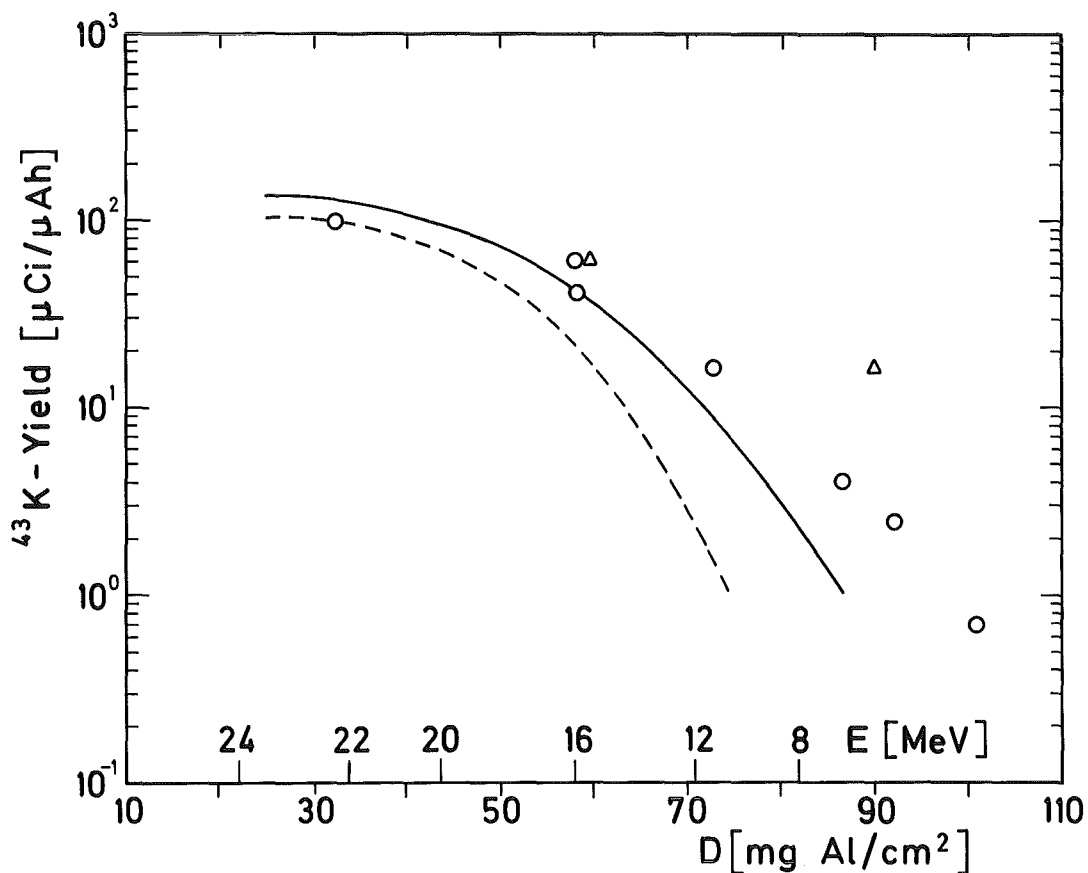


Abb. 1: Dependence of the ^{43}K yield on the thickness of the Al absorber and on the average projectile energy. The values reported by Clark et al. ¹⁾ (—) and Tanaka et al. ⁴⁾ (-----) are also shown

References

- 1) J.C. Clark, M.L. Thakur, I.A. Watson; Int. J. Appl. Radiat. Isotopes 23 (1972) 329
- 2) N.A. Dyson, P.E. Francois; Int. J. Appl. Radiat. Isotopes 7 (1959) 150
- 3) F. Michel, H. Münzel; KFK-Ext. 10/76-1
- 4) S. Tanaka, M. Furukawa, T. Mikumo, S. Iwata, M. Yagi, H. Amano; J. Phys. Soc. Japan 15 (1960) 592

3.4 Materials Research

3.4.1 Helium Bath Irradiation Facility for Superconductors

H. Becker, P. Maier, J. Pytlik, H. Ruoss, E. Seibt, Institut für Experimentelle Kernphysik der Universität und der Gesellschaft für Kernforschung mbH., Karlsruhe

To study the effects of low temperature irradiation on technological superconductors, a helium bath irradiation facility has been installed at the Karlsruhe cyclotron. Results of NbTi and superconductors of A15 crystal structure (V_3Ga , Nb_3Sn) have been obtained with respect to the dependence of their critical current densities j_c and their transition temperatures T_c on 50 MeV deuteron irradiation and successive annealing.

Introduction

The helium bath irradiation facility ¹⁾ installed at the Karlsruhe cyclotron was designed for testing superconductors during and after irradiation with the extracted beam provided by the cyclotron (25 MeV per nucleon) while they are immersed in liquid helium. The operating conditions of superconducting devices subjected to strong nuclear radiation, for example beam guiding superconducting magnets in accelerators or toroidal coils in planned fusion reactors, are thus simulated. In the latter, the maximum total flux to be expected in an operation period of 10 years amounts to about 10^{19} cm^{-2} (14 MeV neutrons) which may be simulated by 10^{18} cm^{-2} (50 MeV deuterons). The radiation-induced defect clusters and the originally present metallurgical structures directly affect the maximum current density j_c , while the transition temperature T_c will be altered by the changed electronic properties of the superconductor. Therefore it is expected that these studies will lead to a better understanding of the principles, e.g. pinning mechanisms, that are responsible for the macroscopic qualities of different superconductors ($NbTi$ ²⁾, V_3Ga ³⁾, Nb_3Sn ⁴⁾).

Experimental Set-up

To permit irradiation and measurements in the temperature range of liquid helium and above 4.2 K without disassembly or warming-up of the samples, the helium bath irradiation cryostat is equipped with a special beam window system (see Fig. 1). During irradiation of the sample, the charged particle beam passes the gap between the inner windows which is filled with liquid helium. The particle flux is adjusted to yield temperatures of the sample equal to T_c , which are easily monitored. At 50 MeV deuteron irradiation the beam current was typically 1 μ A at 10 mm diameter. Between irradiation periods the samples are lowered into the superconducting solenoid (maximum B = 7.5 T) for critical current and magnetization measurements. The transition temperatures may be recorded with a resistive method.

There are special sample holders which permit stationary currents up to 2000 A. The cryogenic supply with helium recovery permits continuous irradiation.

Measurements

The following properties of irradiated superconductor samples are measured as a function of integrated particle fluxes Φt or absorbed doses D: (1) the critical current density j_c (B), (2) the magnetization M (B) at 4.2 K, (3) the transition temperature T_c and (4) the normal state resistivity ρ_n .

After irradiation there will be periods of stepwise annealing at different temperatures up to 1000^o. After each step the superconducting properties are measured at 4.2 K. The superconducting wire samples (\approx 1 mm in diameter, length 28 mm) are of considerable internal complexity. In the case of a diffusion processed^{5,6)} Nb₃Sn composite wire (FURUKAWA, Japan) 6 single wires each containing 55 Nb₃Sn filaments are stranded around a central stabilizing wire of tungsten. The characteristic effect of irradiation with 50 MeV deuterons at 18 K on j_c of this Nb₃Sn composite wire is shown in Fig. 2. The irradiation data of a standard NbTi sample (VAC/SIEMENS) are included for comparison.

The critical current densities are normalized to the values before irradiation and taken at $B = 7$ T. At a total integrated flux of $0.7 \cdot 10^{18} \text{ cm}^{-2}$ the reduction of j_c in Nb_3Sn is 92 %, which compares to only 10 % in NbTi . This sharp decrease in critical properties seems to be a common effect in superconductors of A15 crystal structure ^{7,8}). This different irradiation resistance is an important result for technical applications in magnet building.

References

- 1) H. Becker, H.K. Katheder, E. Seibt, S. Steinacker; KFK 1684 (1972) Karlsruhe
- 2) K. Wohlleben; J. Low Temp. Phys. 13 (1973) 269
- 3) K.-R. Krebs, P. Maier, E. Seibt; KFK 1996 (1974) Karlsruhe
- 4) H. Bauer, E.J. Saur, D.G. Schweitzer; J. Low Temp. Phys. 19 (1975) 171
- 5) M. Wilhelm, E. Springer; Z. Naturforsch. 27a (1972) 1462
- 6) Y. Furuto, T. Suzuki, K. Tachikawa, Y. Iwasa; Appl. Phys. Lett. 24 (1974) 34
- 7) E. Seibt; Appl. Supercond. Conf. 1974, Oakbrook, IEEE Transact. Magn. 11 (1975) 174
- 8) D.M. Parkin, A.R. Sweedler; Appl. Supercond. Conf. 1974, Oakbrook, IEE Transact. Magn. 11 (1975) 166

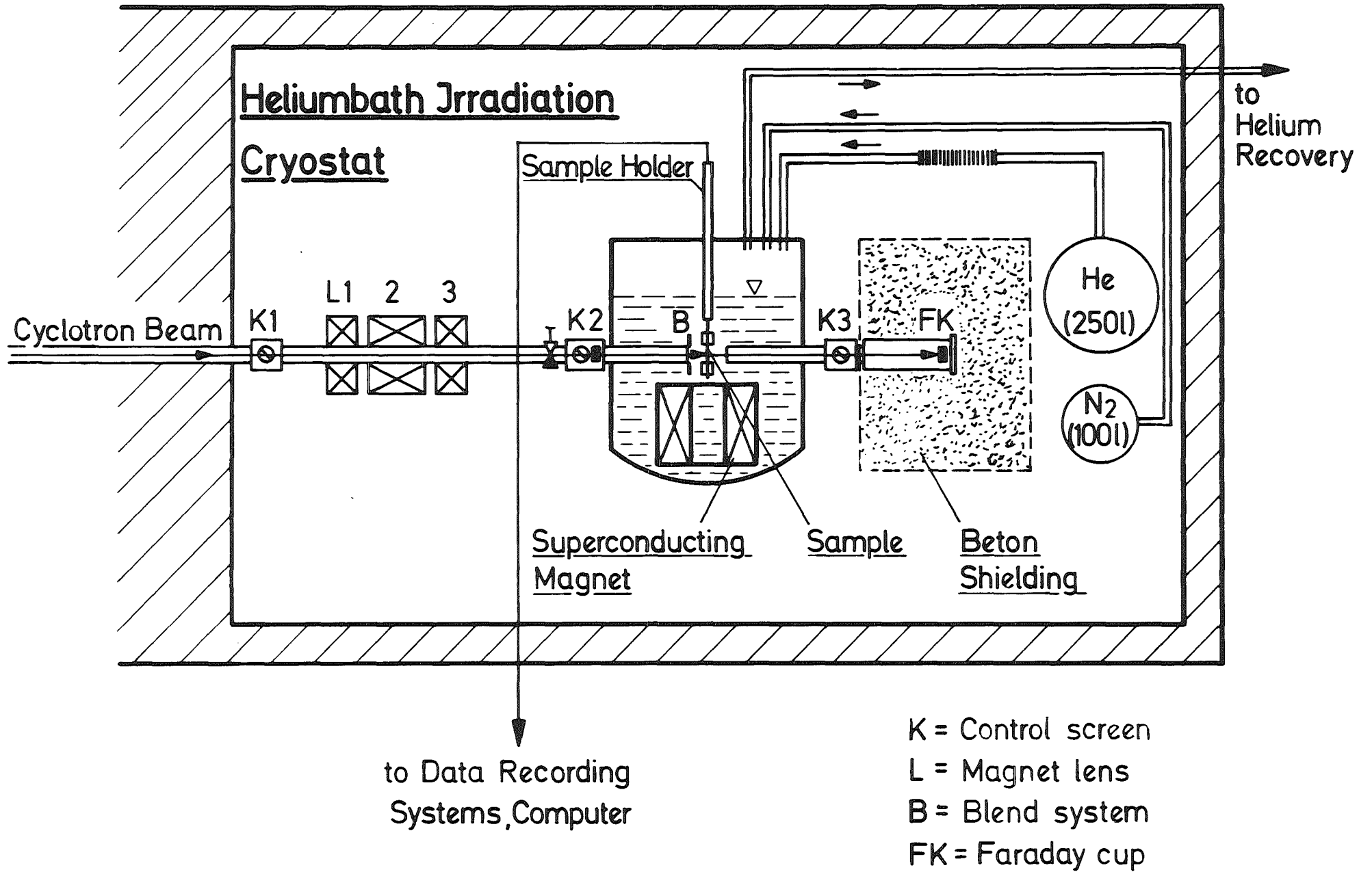


Fig. 1: A schematical view of the helium bath irradiation facility at the Karlsruhe cyclotron

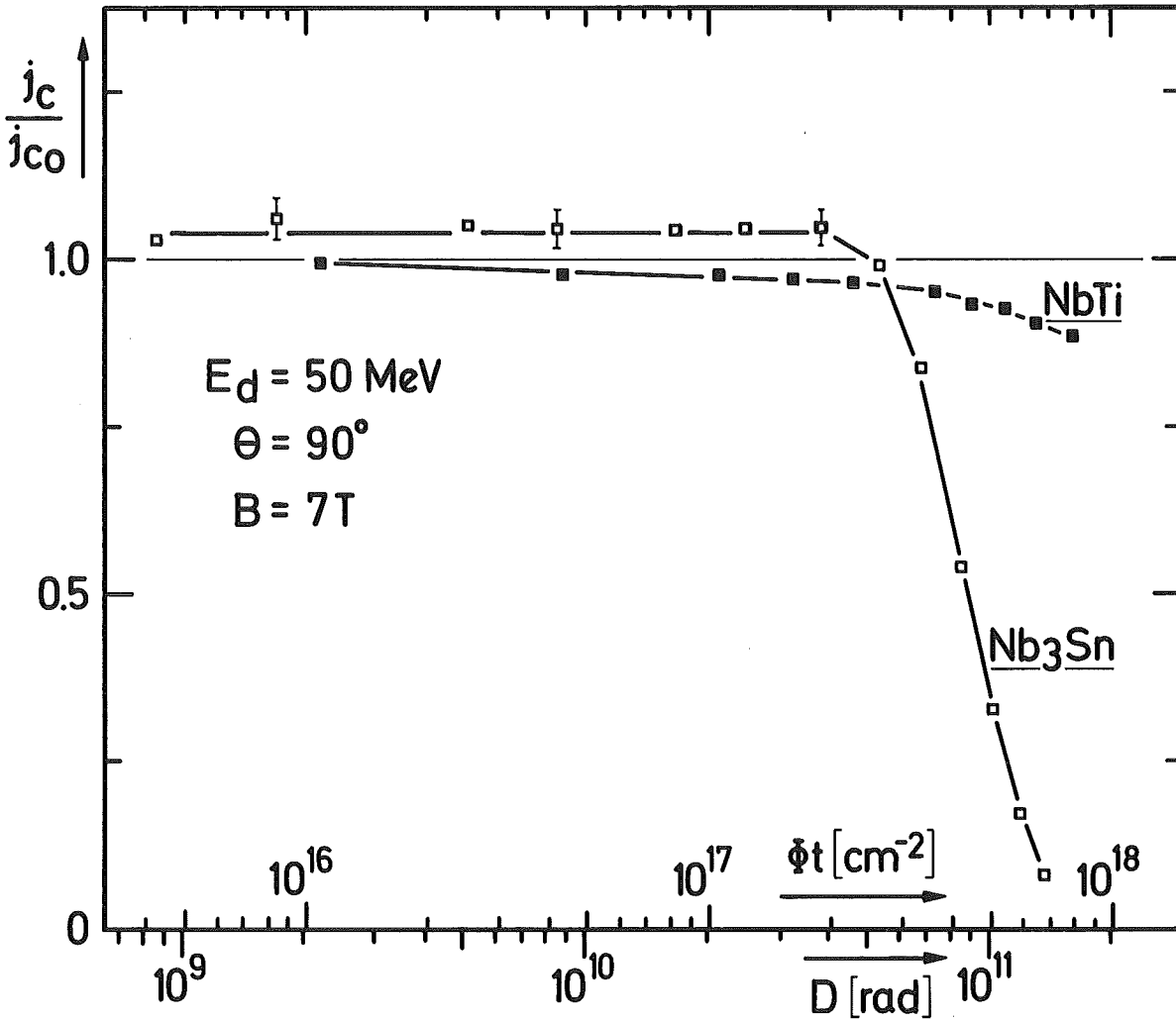


Fig. 2: Irradiation effects on the normalized critical current density j_c/j_{c0} of two superconducting composite wires, NbTi (F 60-133, VAC/SIEMENS) and Nb₃Sn (FSW-NS-1S, FURUKAWA, Japan), versus integrated deuteron flux Φt (absorbed dose D) at transvers induction $B = 7 \text{ T}$

3.4.2 Apparatus to Study Irradiation-Induced Creep with a Cyclotron

K. Herschbach and K. Mueller

Institut für Materialforschung II, Kernforschungszentrum Karlsruhe

An important aspect in the design of economical Fast Breeder fuel elements is the question of dimensional stability of the cladding material. Two aspects in this context which concern the designing engineer are swelling and irradiation-induced creep under the intense neutron irradiation in the reactor since both phenomena result in a restriction of the coolant flow and may therefore force the exchange of the fuel elements even though not all the fuel may have been used up. Creep experiments in the reactor are rather expensive and difficult to do; on the other hand one would like to study in-pile creep in more detail in order to get a better understanding of the microscopic processes involved. In the following an apparatus is described which allows us to simulate in-pile creep with a cyclotron provided that particles of high enough energy are available and that the sample material is compatible with liquid Na used as a coolant. The basic feature of the creep capsule, shown schematically in Fig. 1, is a chimney which encloses the specimen. A heater below the specimen provides the heat necessary to keep the temperature of the Na-bath. The sodium flows upwards due to convection caused by a kind of chimney effect, and leaves the chimney through slots provided above the sample. The specimen temperature can therefore be kept within close limits if a very fast temperature controller is employed. Both convection as well as conduction will carry away any unwanted heat. As can be seen from Fig. 1 the chimney is part of the power train which is otherwise quite conventional. The specimen elongation is measured with a Linear Variable Differential Transformer. Of course, in order to get a high accuracy of the strain measurements a number of precautions were found to be necessary. To facilitate irradiation use is made of the fact that 52 MeV deuterons can penetrate quite a bit of material. The beam entrance window is made of Ni, for safety reasons 1 mm thick. The energy loss in this window is 15 MeV. The beam is further downgraded in the liquid Na

and hits the sample with an energy of appr. 15 MeV. The distance between Ni window and specimen can be adjusted via a kind of micrometer device, the sealing of the capsule being provided by the bellows shown. Needless to say that because of the large amount of liquid Na involved, which will be very radioactive after irradiation, the outmost care and very stringent inspection requirements have to be employed when the creep capsule is being fabricated. The capsule has been tested successfully and first results are presently being obtained.

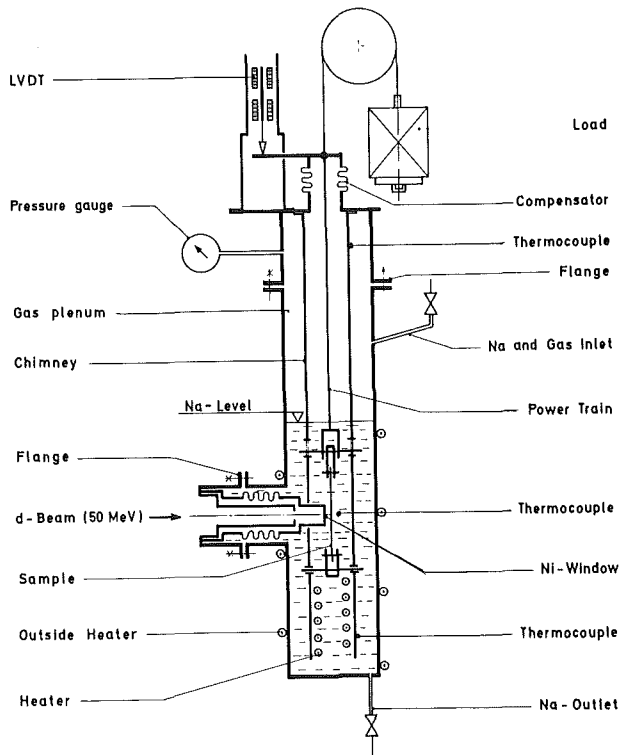


Fig. 1 Schematic diagram of the creep capsule

3.4.3 Radiation Damage Experiments

D. Kaletta, G. Przykutta

Institut für Materialforschung II, Kernforschungszentrum Karlsruhe

Goal of the irradiation experiments with 104 MeV alphas

The generation of helium by (n, α)-processes in the first wall of a fusion reactor or in a fuel device of a fast breeder reactor is one of the most important radiation damages. The existence of helium

- (i) influences the nucleation of voids dominantly, which have lead to the voidage problems of nuclear materials, and
- (ii) causes the high-temperature embrittlement of nuclear materials by the formation of helium clusters and/or helium bubbles. High-temperature embrittlement determines the maximum stresses to be applied to the fuel devices.

The goal of this investigation is to study the mechanism of high-temperature embrittlement, i.e. the influence of helium on mechanical properties at temperatures given by the reactor operation.

Experimental equipment

To study the phenomena of high-temperature embrittlement one needs an accelerator system generating high-energy helium particles which penetrate bulk samples of thicknesses between 200 and 500 μm . Furthermore the beam current density must be high enough, i.e. $\geq 3 \mu\text{A}/\text{cm}^2$, to ensure the implantation of high amounts of helium (1 - 100 at. ppm) in times being realistical.

The target irradiation itself takes place in a high-vacuum target chamber designed for this type of experiments. The core of the chamber is a target holder which can be held at constant temperatures up to 650^oC (s. fig.). The azimuthal as well the axial movements of the target holder were controlled by stepping motors. A detector and monitor system, being under investigation, is capable of giving information of the local beam current at each point in the x-z plane of the sample area irradiated. A water-cooled rotating moderator disc of varying thickness reduces the

input ion energy of 104 MeV down to 1 MeV periodically to allow a helium deposition at all depths of the sample.

Results

The α -irradiations were done for pure vanadium and several binary and ternary vanadium alloys. The samples irradiated were investigated by tensile testing machines working at elevated temperatures. The influence of the helium implanted on the materials depends on the yield points of the materials. As further shown there is a strong correlation between the implantation dose and the irradiation temperature for the formation of He-clusters and bubbles observed by transmission electron microscopy techniques. Due to this strong correlation the experimental work is extended to irradiations at higher temperatures.

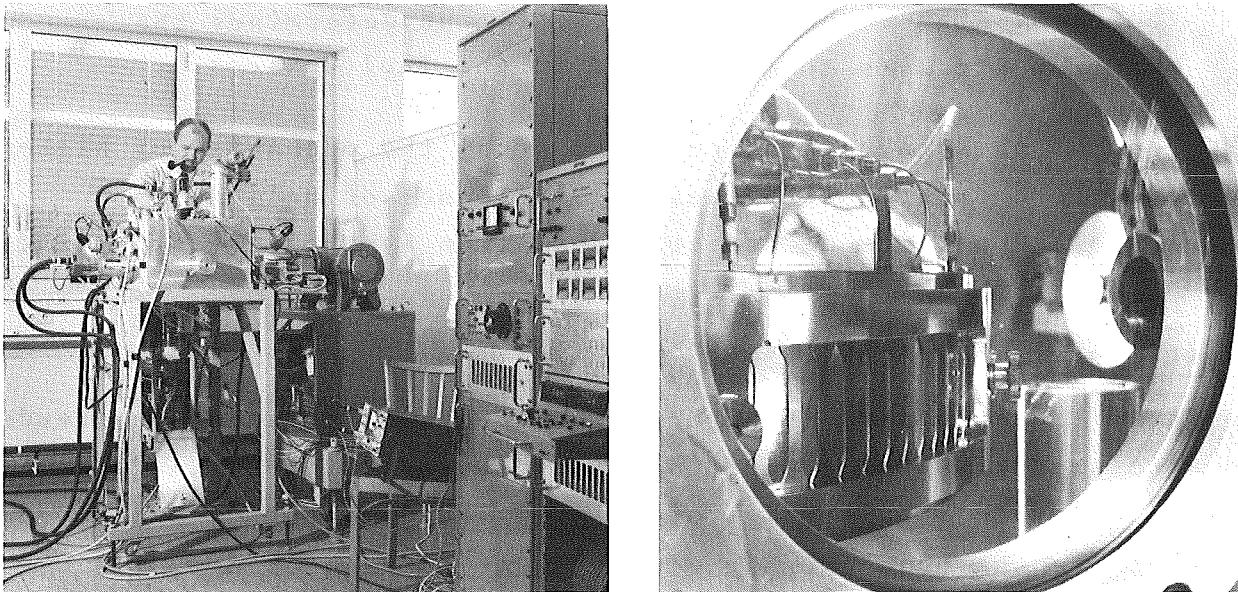


Fig. 1 High-vacuum target chamber for the implantation of 104 MeV helium-ions. The right picture shows the target holder which can be held at constant temperatures up to 650°C.

3.5 Nuclear Chemistry

3.5.1 Studies of the independent yields of ^{148m}Pm and ^{148g}Pm and their isomer ratio in α -particle induced fission of ^{232}Th

D.C. Aumann, W. Gückel, E. Nirschl and H. Zeising

Institut für Radiochemie der Technischen Universität München

The independent yields of 41.3 d ^{148m}Pm and 5.37 d ^{148g}Pm were measured in the fission of ^{232}Th induced by α -particles of energies 27 - 45 MeV. 20 - 100 μ thick thorium foils were irradiated in the internal beam of the Karlsruhe Cyclotron. The beam intensity was 20 μA , the irradiation time 10 or 20 hours. After irradiation the foils were shipped to Munich.

The Pm-isotopes were separated from Thorium and the fission products by radiochemical means. The separation procedure consisted essentially of a separation of the rare earths from thorium and all the other fission products and two separations of the individual rare earths by cation exchange using a solution of α -hydroxyisobutyric acid as eluent.

The Pm fractions were counted on a coaxial Ge(Li)-gamma spectrometer, which was calibrated with a set of standard sources. The activities of ^{148g}Pm and ^{148m}Pm were determined by measuring the photopeaks of the 1465 keV γ -line and of the 629.9 keV and the 725.6 keV γ -lines, respectively.

The independent yields of the two isomers of ^{148}Pm in the α -induced fission of ^{232}Th as a function of the α -particle energy is given in Fig. 1. The experimentally determined isomer ratios of ^{148}Pm are shown in Fig. 2.

The isomer ratios will be used for calculations of the spin distribution of the primary fission fragments. The independent fission yields will give some insight into the variation of Z_p , the most probable charge of a mass chain, with excitation energy of the fissioning compound nucleus.

Fig. 1: Independent yields of ^{148m}Pm and ^{148g}Pm in α -particle induced fission of ^{232}Th

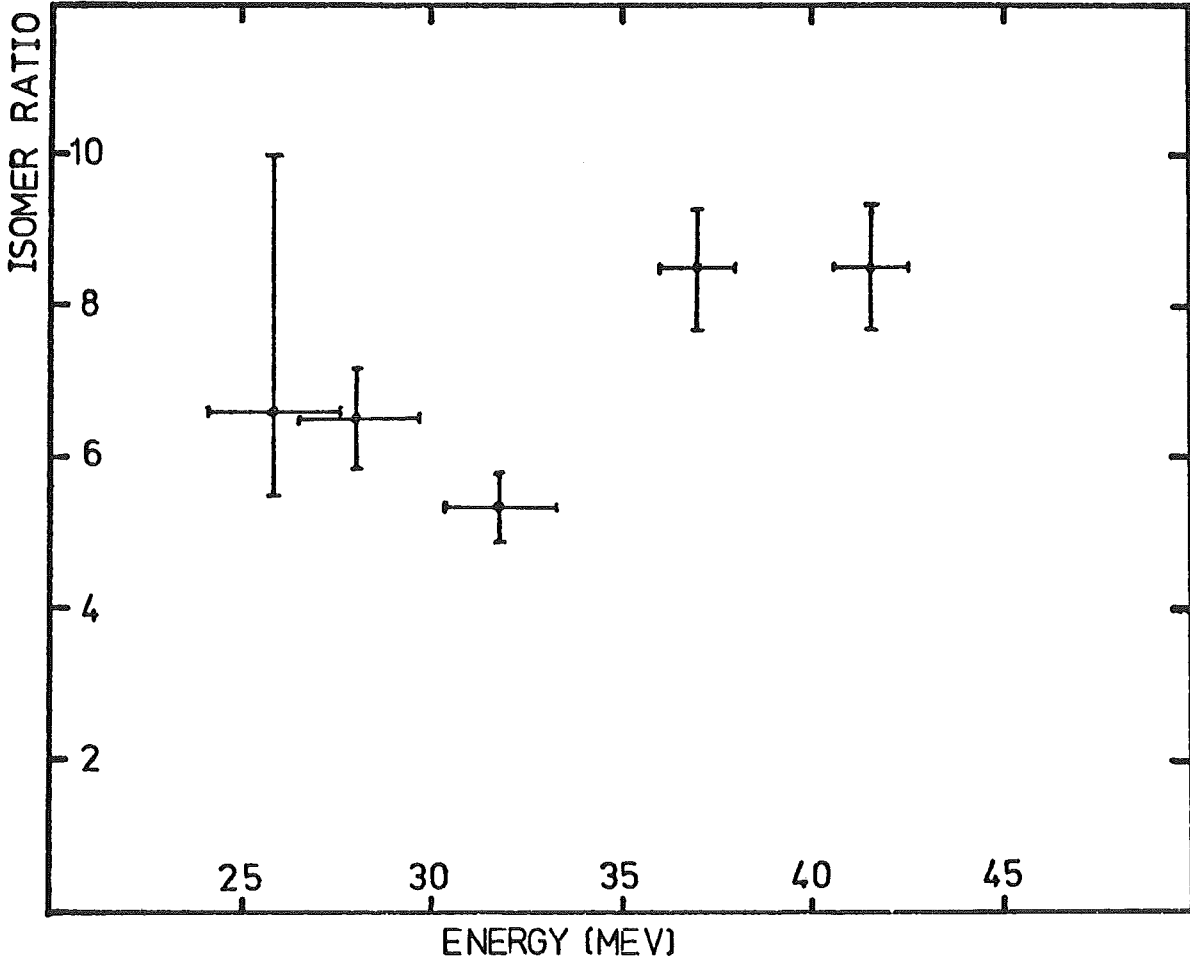
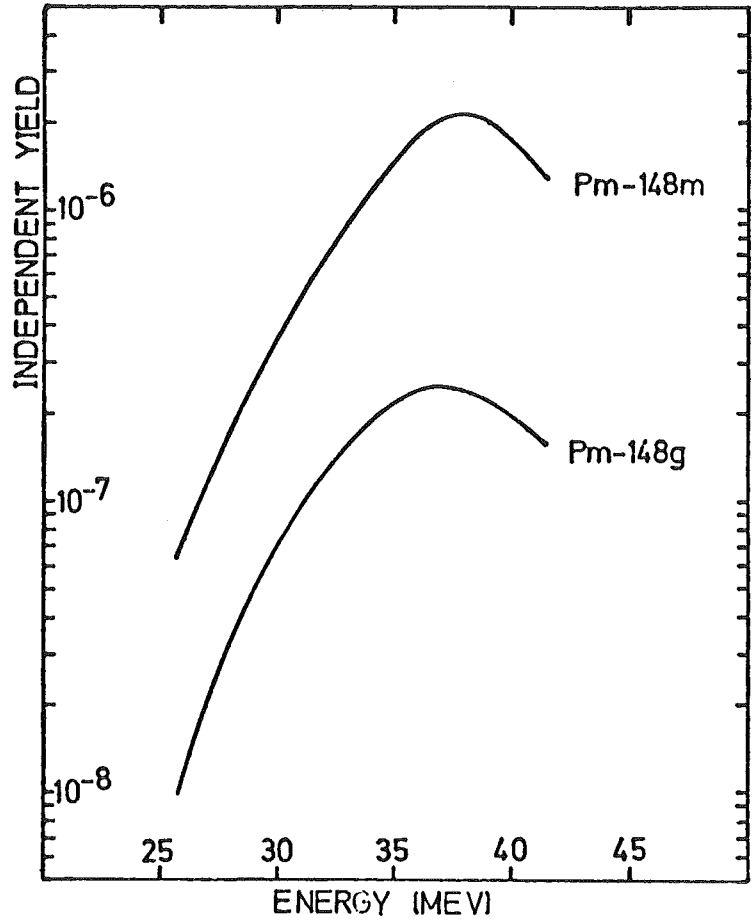


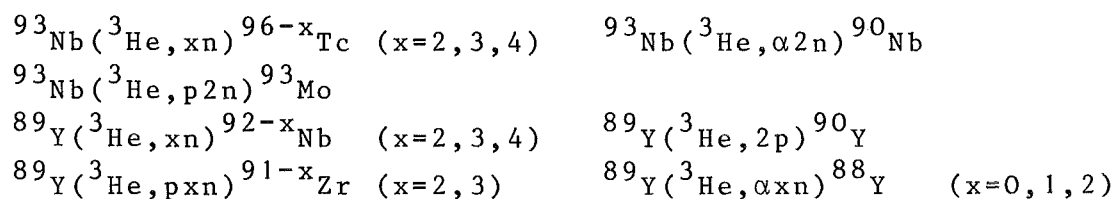
Fig. 2: Isomer ratio of ^{148}Pm formed in α -particle induced fission of ^{232}Th

3.5.2 Excitation functions of ^3He -reactions with Y and Nb

S. Flach and H. Münzel

Institut für Radiochemie, Kernforschungszentrum Karlsruhe

Despite the fact that the number of machines for accelerating ^3He did increase considerably in the last years there were up to now only rather few excitation functions measured for ^3He -reactions. Consequently, the half empirical systematics of excitation functions ¹⁾ published in 1974 did contain for many ^3He -reactions only rough guesses. Therefore we have in the frame of new research program determined for projectile energies up to 40 MeV the excitation functions for the following reactions ³⁾.



In figure 1 some of the results are shown. The measured values are compared with calculated cross sections using a combination of the compound- and the precompound-reaction model. The agreement between experimental and calculated values is not very satisfactory (see figure 2). In general the emission of protons is overestimated, which is probably due to the magic number $N = 50$.

References

- 1) H. Münzel, J. Lange, K.A. Keller; Landolt-Börnstein: Zahlenwerte und Funktionen aus Naturwissenschaften und Technik, N.S. Gruppe 1, Bd. 5c; Springer Verlag, Berlin, Heidelberg, New York, 1974
- 2) J. Lange, H. Münzel, K.A. Keller, G. Pfennig, *ibid.*, Bd. 5b; Springer Verlag, Berlin, Heidelberg, New York, 1973
- 3) S. Flach, Thesis, University Karlsruhe, 1976

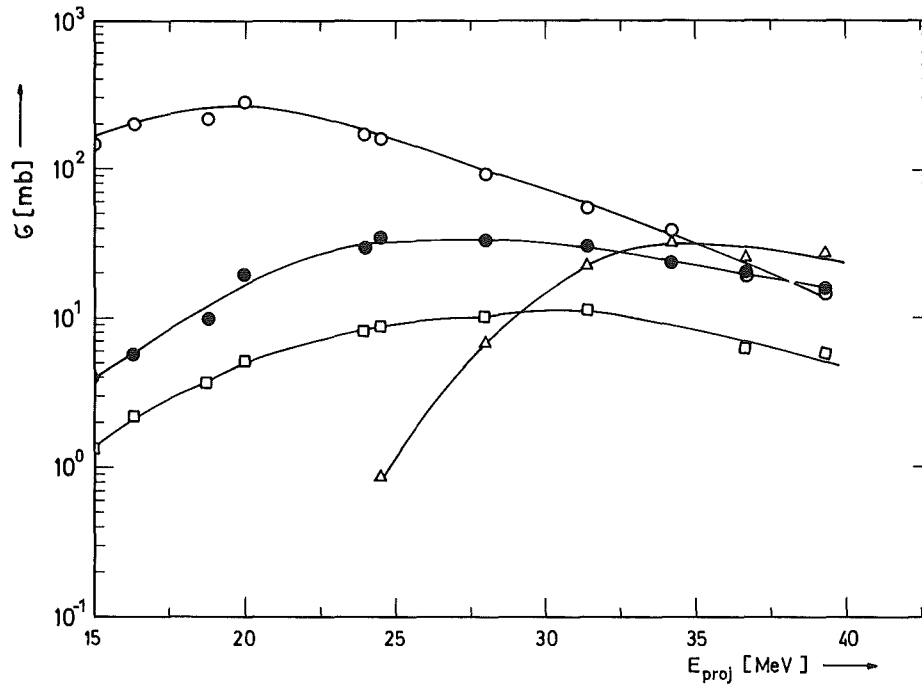


Fig. 1: Excitation functions for the following reactions:
 ○: $^{89}\text{Y}(^3\text{He}, 2n)^{90\text{m}+g}\text{Nb}$ □: $^{89}\text{Y}(^3\text{He}, 2p)^{90\text{m}}\text{Y}$
 ●: $^{89}\text{Y}(^3\text{He}, \alpha n)^{87\text{m}}\text{Y}$ Δ: $^{89}\text{Y}(^3\text{He}, \alpha 2n)^{86\text{m}}\text{Y}$

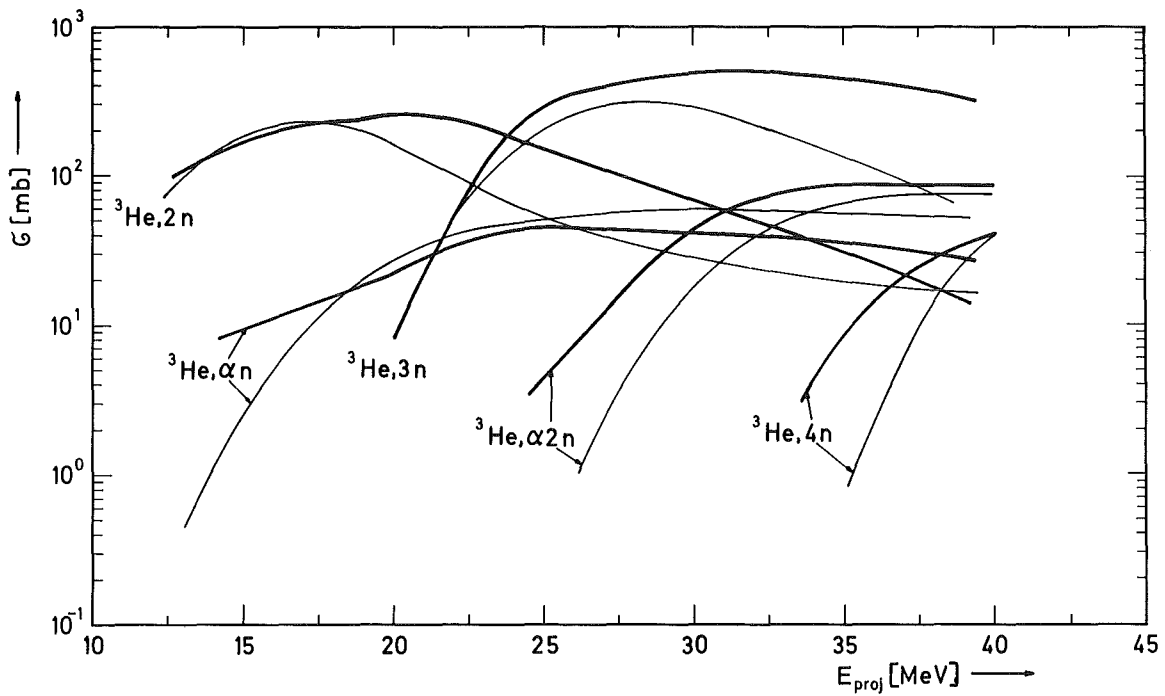


Fig. 2: Comparison of experimentally determined excitation functions (—) for ^3He -reactions on ^{89}Y with calculated curves (—)

3.5.3 Model Experiments Concerning the Separation and Identification of Short-lived Elements Specially with Regard to Transactinides

W. Fröschen, I. Dreyer, G.K. Wolf, Universität Heidelberg

The taking up of operation at the Heavy Ion Accelerator UNILAC of the GSI (Gesellschaft für Schwerionenforschung) in early 1976 in Darmstadt will give new impulses to the discussions on the existence and life time of the superheavy elements which have been going on for years. "Super heavies" are artificial elements representing an extension of the known periodic system of elements beyond the actinides.

Previous experiments carried out at the research centres of Berkeley, USA, and Dubna, USSR, with the intention to produce nuclei of this kind - especially in the region of the so-called "stability island" around $Z = 114$ which on the basis of theoretical calculations are expected to be relatively stable - have up to now not been successful. This failure might possibly be explained by the use of non-optimal projectile/target combinations and too low beam intensities.

The Heavy Ion Accelerator UNILAC is the first plant by which it will be possible to produce heavy ion beams up to uranium with a variable energy up to 7 MeV/nucleon and an intensity of 10^{12} to 10^{13} particles/sec. On the basis of these conditions it should be possible to prove the existence of new elements beyond the actinides or at least to set up new limits of detection.

Because of the small number of nuclei that can be created in such experiments, and because of their short life time it is required to have highly specialized apparatus conditions at the accelerator and utmost rapid and efficient methods for separating and identifying the products by making use of their different chemical and physical properties which are deduced from the homology principles of the periodic system.

Separation and characterization of the nuclei which must precede their identification may e.g. be achieved by chemical separation methods in the gas and liquid phase or solid state reactions.

It was the objective of our group to develop relevant model reactions - concentrating our attention especially on selective solid state reactions - and to develop an appropriate apparatus for ON-LINE operation at the Heavy Ion Accelerator.

Fig. 1 is a schematic representation of the principle of the procedure.

The compound nuclei created in the high temperature target leave this target in the direction of the beam due to the momentum transferred to them by the nuclear reaction process. They are slowed down and collected by a catcher which is designed such that the nuclei either react selectively in a characteristic manner giving a volatile chemical compound or in the case of volatile elements remain in elementary form. The catcher is removed from the beam area of the accelerator and heated. The element of interest or the compound formed due to the chemical reaction with the catcher are then evaporated and condensed selectively. Subsequently the condensation area is investigated for spontaneous fission and specific α -events.

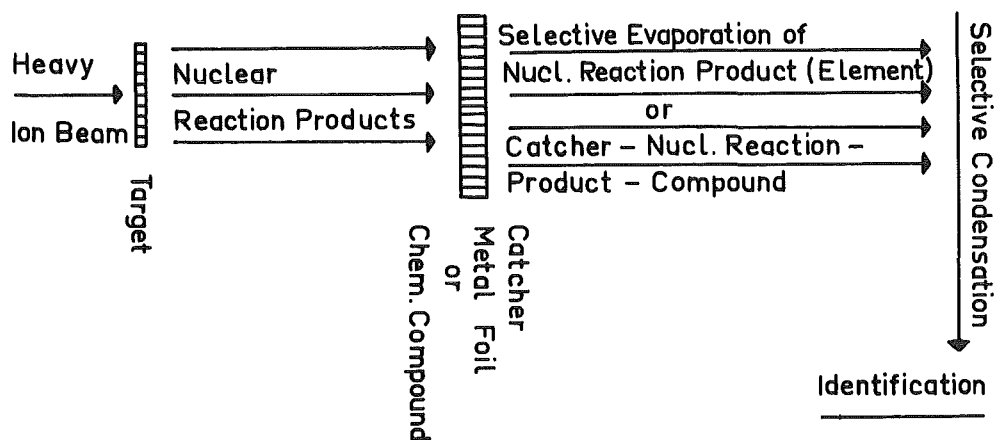


Fig. 1: Rapid separation and identification of nuclear reaction products

For this purpose an apparatus was constructed which allows the irradiation of up to 60 samples at liquid nitrogen temperature using an automatic sample change. After irradiation the samples are automatically taken out of the high vacuum region of the accelerator via a vacuum gate system. They are then transported by means of a pneumatic tube system into a neighbouring laboratory where they can be heated in a quartz evaporation apparatus up to about 1.000°C (and if necessary chlorinated under flowing CCl_4). The vapour condensing on a cooled aluminium tape is conducted either continuously or discontinuously to a detector system.

Both, method and apparatus were examined in a series of test experiments, partly at the Emperor Tandem Accelerator of the Heidelberg MPI für Kernphysik, partly at the Karlsruhe cyclotron. These tests proved to be successful.

At the cyclotron model reactions were carried out using known chemical homologues of the elements in question. We were especially interested in the elements $Z = 104$, i.e. eka-hafnium and $Z = 112$, i.e. eka-mercury, which presumably will have very similar chemical properties as hafnium and zirconium on the one side and mercury and cadmium on the other.

For this purpose SrCl_2 tablets were activated at the Karlsruhe cyclotron by a α -particle beam according to $\text{Sr}(\alpha, xn)\text{Zr}$ and silver and gold foils by deuterons according to $\text{Ag}(\text{Au}) (\alpha, xn) \text{Cd}(\text{Hg})$. The SrCl_2 tablets and the Ag and Au foils were to simulate the catchers for the heavy ion reaction products, whereas the radioactive atoms of Zr, Cd, and Hg created by the activation process were to simulate the nuclear reaction products collected by the catchers.

According to our method we intended for selective separation to make use of the different volatility of the elements or compounds examined. Therefore, we investigated their evaporation behaviour and yield as function of the time. Fig. 2 shows the principle of the experimental arrangement used. By means of this set-up it is possible to evaporate Zr under chlorinating conditions in flowing CCl_4 -Ar in the form of ZrCl_4 out of the SrCl_2 matrix. Cd and Hg evaporate from metal catchers in elementary form without the presence of carrier gas. The vapours condense above the furnace at a cooled area of the quartz tube. At this point the increase

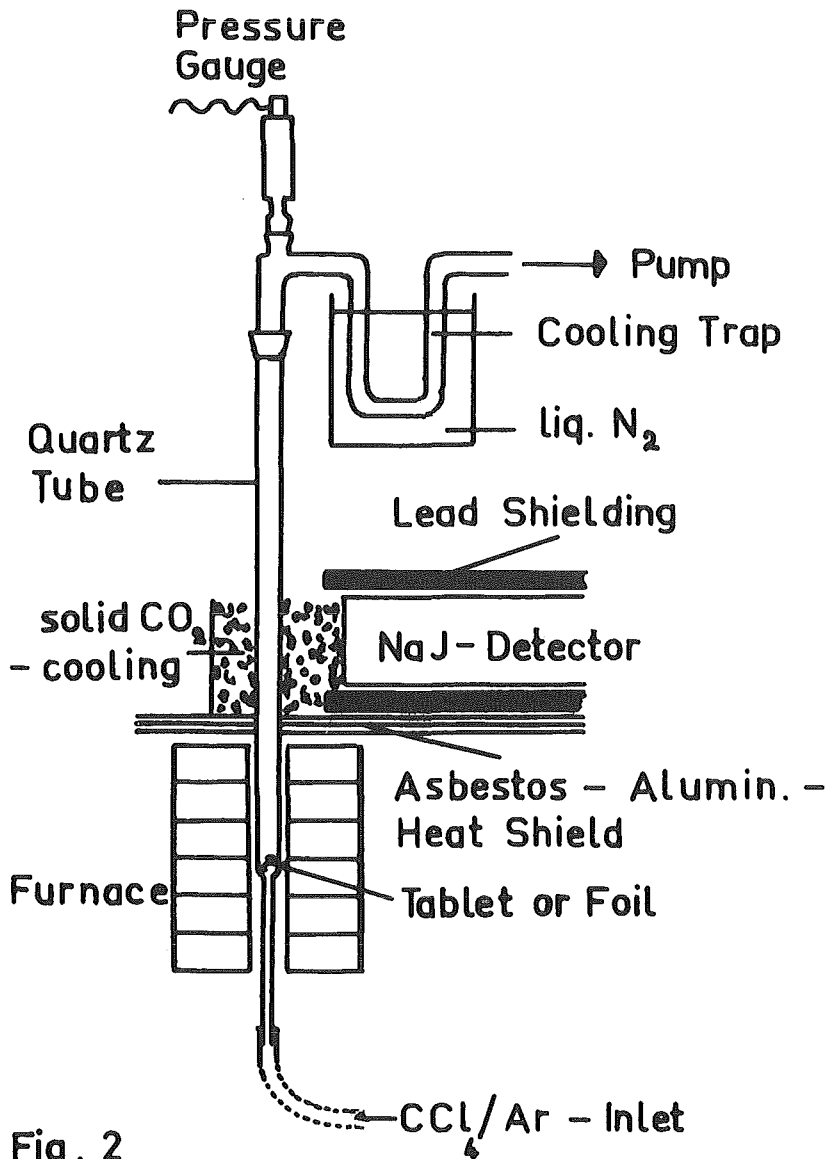


Fig. 2

Evaporation - Condensation - Device

of the γ -activity (characteristic for the nuclide in question) is measured with a NaJ scintillation detector.

The time varying evaporation behaviour of the different systems is generally compared on the basis of the period in which half of the original activity has evaporated.

The "half life" was shown to be about ~ 60 sec for Zr at 1.000°C , about 45 sec for Cd and about 15 sec for Ag at 900°C . The yield was 90 % in the case of Zr (evaporated as ZrCl_4) and 100 % in the cases of Cd and Hg (evaporated in elementary form) ⁴).

This gives rise to the question to what extent the activity present in vapour condenses on a defined (cooled) area. The problem was investigated by examining the condensation behaviour of astatine. Astatine was chosen because it is one of the heaviest of the volatile elements, easily obtainable by α -particle irradiation of bismuth in the cyclotron and easily detectable due to its γ -radiation.

It was evaporated out of molten Bi in a glass apparatus at 400°C and then conducted together with flowing He through a nozzle on two cooled Al or Au foils of about 1 to 2 cm². The yields of the condensation on these foils were examined as a function of gas flow, nozzle opening and nozzle/condensation area distance. With a distance ranging from 0.5 to 0.2 cm and gas flow rates ranging from 3 / min to 0 the yield varied between 10 and 90 %.

Due to the preliminary experiments carried out at the Karlsruhe cyclotron and the Heidelberg Max-Planck-Institut für Kernphysik it has been possible to simulate the conditions of heavy ion reactions and to improve the apparatus parameters and separation methods required for the future search for new transactinides.

References

- 1) S.G. Nilsson, C.F. Tsang; Nrd. Phys. A131 (1969) 1, A140 (1970)289
- 2) GSI-J-1-75, Nov. 75, S. 58
- 3) GSI-J2-74, Nov. 74, S. 114
- 4) J. Römer, Dissertation 1976, Universität Heidelberg

3.5.4 A Nondestructive Determination of P, Ca and K in Soil by Means of α -Particle Activation

C.C. Dantas, P. Misaelides, Institut für Radiochemie, Kernforschungszentrum Karlsruhe

Introduction

In a multielemental analysis by reactor neutron activation P can be determined only in very favourable cases. By thermal neutron activation only ^{32}P , a pure β^- emitter, is produced. An alternative for the P determination is the $^{31}\text{P}(n,\alpha)^{28}\text{Al}$ reaction. In soil samples, where Si is a major constituent element, an interference to the above reaction will be present due to the $^{28}\text{Si}(n,p)^{28}\text{Al}$ reaction.

Investigating the possibilities to extend the instrumental analysis of soil, an attempt was made to use the $^{31}\text{P}(\alpha,n)^{34\text{m}}\text{Cl}$ reaction. This reaction leads to a sensitive determination of P, as it is already described by Vis and Verheul ¹⁾ for water samples analysis.

By the α -activation besides P a reliable detection of Ca and K was also obtained.

Experimental

The samples were irradiated as pressed pellets wrapped twice in 30 μ thick Al foil (99.999 % pure). The internal beam of the isochronous cyclotron of the Nuclear Research Centre Karlsruhe was used for the irradiations. The energy of the incident beam was fixed at 20 MeV, the beam current at 0.5 μA and the irradiation time at 5 min. The energy of the α -particles hitting the mineral material was 16 MeV due to the energy loss in the Al foils.

The γ -counting of the irradiated samples was performed by means of a 42 cm^3 Ge(Li) detector, with a resolution of 1.85 keV for the 1.33 MeV ^{60}Co radiation, coupled to a 4096-channel analyser.

Method

The determination of P, Ca and K was carried out by means of the following nuclear reactions: $^{31}\text{P}(\alpha, n)^{34\text{m}}\text{Cl}$, $^{41}\text{K}(\alpha, n)^{44}\text{Sc}$ and $^{40}\text{Ca}(\alpha, p)^{43}\text{Sc}$ respectively. By the chosen irradiation conditions the activities of the also induced interfering reactions could be neglected. The data for the nuclear reactions are given by ²⁾.

For the irradiations the thick target method was used in order to eliminate the errors due to the thickness of the target. The energy loss of the α -particles in Al-foil and the range in the target was calculated by aid of tables given by Williamson and Boujot ³⁾. The irradiations and counting conditions were chosen by preliminary irradiations.

Nb was chosen as flux monitor by means of the $^{93}\text{Nb}(\alpha, n)^{96\text{g}}\text{Tc}$ reaction.

The calibration curves for P, Ca and K were obtained by using geological standards. The concentration of the elements in the soils was determined by interpolating the activity of the element divided by the activity of the monitor on the corresponding calibration curve. A reproducibility of 5 % was found among the analyzed soil samples.

The results of the determination of P, Ca and K in the different soils are listed in Table I. In the same table the results of the K determination by α -particle and thermal neutron activation can be compared.

Using the formulas given by Currie ⁴⁾ and the tables of the ref. (3) a calculation of the lower limits of concentration and an estimation of detection limits were carried out. These results are given in the Table II.

Soil	P [%]	Ca [%]	K [%]	
			this work	Thermal neutron activation
1	0.170	1.810	4.10	4.80
2	0.040	0.039	3.10	3.38
3	0.014	0.043	5.20	4.52
4	0.030	0.236	4.00	3.93
5	0.031	0.050	5.30	6.60
6	0.020	0.044	4.50	3.70
7	0.064	0.034	3.30	2.89
8	0.050	0.203	0.34	0.41
9	0.024	0.156	0.27	0.27

Table I: Concentration of the elements in the soils determined by α -particle activation

Element	Detection limits [g]	lower limit of concentration [ppm]
P	10^{-7}	30
Ca	$3 \cdot 10^{-7}$	100
K	10^{-6}	400

Table II: Detection limits and lower limit of concentration of the determined elements

References

- 1) R.D. Vis, H. Verheul, J. Radioanal. Chem. 25 (1975) 293
- 2) K.A. Keller, J. Lange, H. Münzel, Q-Values, Landolt-Börnstein: Zahlenwerk und Funktionen aus Naturwissenschaften und Technik, N.S. Gruppe 1, Bd. 5a, Springer-Verlag Berlin, Heidelberg, New York, 1973
- 3) C.T. Williamson, J.P. Boujot, J. Picard, Rapport CEA-R 3042, Centre d'études nucléaires de Saclay 1966
- 4) C.A. Currie; Anal. Chem. 40 (1968) 586

Publications in 1975 using the Karlsruhe Isochronous Cyclotron

NUCLEAR REACTIONS

Gils, H.J.; Rebel, H.;

Empirical Studies of the Folding Model of 104 MeV α -Particle Scattering and Determination of Isoscalar Transition Rates.

Frühjahrstagung DPG, Kernphysik, Den Haag, 7.-11. Apr. 1975,
Verhandlungen der Deutschen Physikalischen Gesellschaft, R.6,
Bd. 10 (1975) S. 745 - 46

Bechtold, V.; Friedrich, L.; Bialy, J.; Junge, M.; Schmidt, F.K.;
Strassner, G.;

Untersuchung von Kernreaktionen am Kohlenstoff mit vektorpolarisierten Deuteronen von 52 MeV.

Frühjahrstagung DPG, Kernphysik, Den Haag, 7.-11. Apr. 1975,
Verhandlungen der Deutschen Physikalischen Gesellschaft, R.6,
Bd. 10 (1975) S. 866

Gils, H.J.; Rebel, H.;

Differences between Neutron and Proton Density RMS-Radii of $^{204,206,208}\text{Pb}$ Determined by 104 MeV α -Particle Scattering.

Symposium on Nuclear Structure: Coexistence of Single Particle and Collective Types of Excitations, Balatonfüred/Hung., September 1-7, 1975

Gils, H.J.; Rebel, H.;

Empirical Studies of the Effective Interaction and of Exchange Effects for the Folding Model Approach of 104 MeV α -Particle Scattering.

KFK-2127 (Mai 1975)

Rebel, H.;

Nuclear Size and Shape Information from Alpha Particle Scattering at 100 MeV.

Symposium on Nuclear Structure: Coexistence of Single Particle and Collective Types of Excitations, Balatonfüred/Hung., September 1-7, 1975

Eyrich, W.; Berg, M.; Hofmann, A.; Rebel, H.; Scheib, U.;

Schneider, S.; Vogler, F.;

$^{24}\text{Mg}(\alpha, \alpha'\gamma)$ Angular Correlation Measurements at 104 MeV as a Test for the Quadrupole Deformation.

4. Internat. Symposium on Polarization Phenomena in Nuclear Reactions, Zürich, August 25-29, 1975

Gils, H.J.;

Experimentelle Untersuchungen der Radiusdifferenzen zwischen Protonen- und Neutronendichteverteilung von $^{204,206,208}\text{Pb}$ und Studien von Oktopolübergangsdichten durch Streuung von 104 MeV α -Teilchen.

Dissertation, Univ. Heidelberg 1975, KFK-2225 (November 1975)

Gils, H.J.; Rebel, H.;
Isoscalar Transition Rates from Folding Model Analyses of (α, α')
Scattering.
Zeitschrift für Physik A, 274 (1975) S. 259-66

Bialy, J.; Junge, M.; Kluge, W.; Matthaey, H.; Schlufte, R.;
Schneider, H.;
Experimental Investigation of the Reaction $dd \rightarrow dpn$ at 52.3 MeV.
Symposium on Few Particle Problems in Nuclear Physics, Tübingen,
May 17-19, 1975

Bechtold, V.; Friedrich, L.; Bialy, J.; Junge, M.; Schmidt, F.K.;
Strassner, G.;
Elastic and Inelastic Scattering of 52 MeV Vector Polarized
Deuterons on ^{12}C .
4. Internat. Symposium on Polarization Phenomena in Nuclear Reactions,
Zürich, August 25-29, 1975

Klewe-Nebenius, H.; Wisshak, K.;
Gils, H.J.; Rebel, H.; Nowicki, G.; Ciocanel, A.; Hartmann, D.;
Deformation of ^{56}Fe from 104 MeV α -Particle Scattering.
Journal of Physics G, Nuclear Physics, 1 (1975) S. 344-57

Mairle, G.; Wagner, G.J.;
The Decrease of Ground-State Correlations from ^{12}C to ^{14}C .
Nuclear Physics A, 253 (1975) S. 253-62

Wagner, G.J.; Doll, P.; Knöpfle, K.T.; Mairle, G.;
Lifetime of Nuclear Hole States Caused by Phonon-Hole Coupling.
Physics Letters, 57 B (1975) S. 413-16

Haase, E.L.;
Large-Area Position Sensitive Time-of-Flight Counters for Neutrons
and Charged Particles.
Journées d'études de Physique Nucleaire a Moyenne Energie, Orsay,
April 12-14, 1975

Schwinn, U; Mairle, G.; Wagner, G.J.; Rämer, Ch.
Proton Pick-up from Nuclei in the Middle of the $1p$ Shell.
Zeitschrift für Physik A, 275 (1975) S. 241-47

SOLID STATE PHYSICS

Fink, J.; Czjzek, G.; Schmidt, H.; Krill, G.; Lapierre, M.F.;
Gautier, F.; Robert, C.;
An Investigation of NiS₂ by ⁶¹Ni-Mössbauer Spectroscopy:
Influences of Vacancies and Copper Impurities.
Discussion Meeting on Magnetic Semiconductors, Jülich, September 29-Okt.1, 1975

Parisot, G.I.; Coey, J.M.D.; Brusetti, R.; Gompf, F.; Czjzek, G.;
Fink, J.;
Electron-Phonon Coupling and the Loss of Magnetism in NiS.
21. Annual Conference on Magnetism and Magnetic Materials, Philadelphia,
Dezember 9-12, 1975

Czjzek, G.; Fink, J.; Schmidt, H.; Krill, G.; Lapierre, M.F.;
Robert, C.; Gautier, F.;
Untersuchung von NiS₂ mit Hilfe der Mössbauerspektroskopie an ⁶¹Ni.
Frühjahrstagung DPG, Festkörperphysik, Münster, 17.-22. März 1975.
Verhandlungen der Deutschen Physikalischen Gesellschaft, R.6,
Bd. 10 (1975) S. 473-74

Czjzek, G.; Fink, J.; Schmidt, H.; Gautier, F.; Krill, G.; Lapierre, M.F.;
Panissod, P.; Robert C.;
An Investigation of Magnetic Structures and Phase Transitions in NiS(2-x)Se(x)
by ⁶¹Ni Mössbauer Spectroscopy.
6. Internat. Conference on Mössbauer Spectroscopy, Cracow/Poland, August
25-30, 1975. Discussion Meeting on Magnetic Semiconductors, Jülich,
September 29 - October 1, 1975

Fink, J.; Czjzek, G.; Schmidt, H.;
Magnetic Hyperfine Interactions of ⁶¹Ni in NiMn Alloys.
6. Internat. Conference on Mössbauer Spectroscopy, Cracow/Poland,
August 25-30, 1975

Hartrott, M. von; Hadijuana, J.; Nishiyama, K.; Quitmann, D.;
Spin Relaxation of Excited Nuclear States: Sn in Liquid In-St Alloys.
2. Spezialized Ampere Symposium, Budapest, August 25-29, 1975

Hartrott, M. von; Nishiyama, K.; Quitmann, D.; Weihreter, E.;
Nuclear Spin Relaxation of Sb in Liquid In(1-x)Te(x).
6. Internat. Conference on Amorphous and Liquid Semiconductors,
Leningrad, November 18-24, 1975

Dimmling, F.; Braeuer, N.; Focke, B.; Kornrumpf, T.; Nishiyama, K.; Riegel, D.;
Lifetime and Magnetic Moment of the $11/2^-$, 731 keV Level in ^{113}Sn .
Zeitschrift für Physik, 271 (1975) S. 103-105

Hartrott, M. von; Hadijuana, J.; Nishiyama, K.; Quitmann, D.;
Spin Relaxation of ^{117}Sb and ^{115}Sn Isomers in Liquid In-Sb Alloys.
Internat. Meeting on Hyperfine Interactions Studied by Nuclear Methods,
Louvain, September 10-12, 1975

Hadijuana, J.; Hartrott, M. von; Nishiyama, K.; Quitmann, D.;
Riegel, D.;
Schweickert, H.;
Nuclear Spin Relaxation of Xenon in Liquid Tellurium.
Frühjahrstagung DPG, Festkörperphysik, Freudenstadt, 1.-5. April 1974
AED-CONF-74-089-051

Riegel, D.;
Relaxation Rates of Excited Nuclei in Liquid Metals.
Physica Scripta, 11 (1975) S. 228-36

Krien, K.; Soares, J.C.;
Hanser, A.; Feuerer B.;
Electric Quadrupole Interaction of the 75 keV State of ^{100}Rh in a
Beryllium Matrix.
Hyperfine Interactions, 1 (1975) S. 41-44

Krien, K.; Soares, J.C.; Vianden, R.; Bibiloni, A.G.;
Hanser, A.;
Temperature Dependence of the Quadrupole Interaction of ^{100}Rh in
a Cd Lattice.
Hyperfine Interactions, 1 (1975) S. 295 - 300

Krien, K.; Soares, J.C.; Freitag, K.;
Tischler, R.; Hanser, A.; Kaufmann, E.N.;
Quadrupolwechselwirkung am ^{100}Rh und ^{181}Ta in Beryllium-Metall.
Frühjahrstagung DPG, Atomphysik, Köln, 24. Febr.- 1. März 1975,
Verhandlungen der Deutschen Physikalischen Gesellschaft, R.6, Ed. 10
(1975) S. 69-70

Feurer, B.; Hanser, A.;
Schnelle elektromagnetische Massentrennung mit interner Chlorierung zur
Herstellung massenreiner Quellen von Seltenerd isotopen mit Halbwertszeiten
 ≥ 1 min. KFK 2146 (Juli 1975)

ENGINEERING

Rüdinger, V.; Schwannecke, H.;
Die Motorische Prüfung des Verschleißschutzes von Schmierölen mit
Hilfe von Radionukliden.
3. DGMK Fachgruppentagung Hannover, 5.-8. Oktober 1975 AED-CONF-75-554-001

Herkert, B.;
Die Aktivierung von metallischen Maschinenteilen mit geladenen Teilchen
zur Durchführung von Verschleißmessungen.
KFK-2096 (Mai 1975)

Herkert, B.;
Verschleißmessungen mit Hilfe von Radionukliden nach dem Durchflußmeßverfahren.
KFK-2182 (Juli 1975)

Katzenmaier, G.; Rüdinger, V.;
The Effect of Surface Profile and Structural Viscosity of the Lubricant
on the Load Capacity of Journal Bearings (Results of Wear Measurements with
Radionuclides).
11. International Congress on Combustion Engines, Barcelona, April 28-May 2,
1975. Vol. 2 Barcelona: o. Verl. 1975, S. 652-72

Gerve, A.; Schatz, G.;
Applications of Cyclotrons in Technical and Analytical Studies.
7. Internat. Conference on Cyclotrons and their Applications, Zürich,
August 19-22, 1975

NUCLEAR SPECTROSCOPY

Klewe-Nebenius, H.; Habs, D.; Wisshak, K.; Faust, H.; Nowicki, G.;
Göring, S.; Rebel, H.; Schatz, G.; Schwall, M.;
The Level Scheme of ^{137}Pr -Evidence for Prolate Nuclear Shape.
Nuclear Physics, A 249 (1975) s. 76-92

Rebel, H.; Faust, H.; Wisshak, K.; Klewe-Nebenius, H.;
Discrimination between prompt $\Delta I=1$ and $\Delta I=2$ Transitions from Conversion
Electron Angular Distributions.
Frühjahrstagung DPG, Kernphysik, Den Haag, 7.-11. April 1975. Verhandlungen
der Deutschen Physikalischen Gesellschaft, R.6, Bd. 10 (1975) S. 744-45

Klinken, J. van; Feenstra, S.J.; Wisshak, K.; Faust, H.;
Mini-Orange Spectrometers.
Frühjahrstagung DPG, Kernphysik, Den Haag, 7.-11. April 1975.
Verhandlungen der Deutschen Physikalischen Gesellschaft, R.6,
Bd. 10 (1975) S. 745 - 46

Hanser, A.; Wisshak, K.; Klewe-Nebenius, H.; Rebel, H.;
Observation of an Enhanced $4^+_{1} \rightarrow 0^+$ Crossover Transition in ^{202}Pb
by Conversion Electron Spectroscopy.
Frühjahrstagung DPG, Kernphysik, Den Haag, 7.-11. April 1975.
Verhandlungen der Deutschen Physikalischen Gesellschaft, R.6
Bd. 10 (1975) S. 856
Physical Review, C12 (1975) S. 338-40

Buschmann, J.; Faust, H.; Klewe-Nebenius, H.; Kropp, J.;
Rebel, H.; Schulz, F.; Wisshak, K.;
In Beam Studies of Ir, ^{197}Au (^6Li , xn+yp) Reactions Induced by
 ^6Li -Ions of up to 156 MeV.
International Symposium on Highly Excited States in Nuclei, Jülich,
September 22-26, 1975

Flothmann, D.; Gils, H.J.; Wiesner, W.; Loehken, R.;
Spectral Shape of the $(7/2^- \rightarrow 5/2^+)$ -Transition in the β -Decay of ^{139}Ba .
Zeitschrift für Physik, A 272 (1975) S. 219-22

Szybisz, L.;
The Half-life of ^{10}Be and the Renormalization of the Axial-Vector
Coupling Constant.
Zeitschrift für Physik, A 273 (1975) S. 277-81

Behrens, H.; Szybisz, L.;
Der Zerfall des T=1-Isospintripletts im A=12-System.
Frühjahrstagung DPG, Kernphysik, Den Haag, 7.-11. April 1975.
Verhandlungen der Deutschen Physikalischen Gesellschaft, R.6
Bd. 10 (1975) s. 804

Behrens, H.; Szybisz, L.;
The Decay of the T=1 Isospin Triplet in A= 2 Systems.
Zeitschrift für Physik, A 273 (1975) S. 177-83

Behrens, H.; Kobelt, M.; Szybisz, L.; Thies, W.G.;
On the $^{11}\text{C} \rightarrow ^{11}\text{B}$ β^+ transition.
Nuclear Physics, A 246 (1975) S. 317-22

Deimling, M.; Neugart, R.; Schweickert, H.;
Spin and Magnetic Moment of ^{25}Na by β -Radiation Detected Optical Pumping.
Z. Physik, A 273 (1975)

Schweickert, H.; Dietrich, J.; Neugart, R.; Otten, E.W.;
Nuclear Spins and Magnetic Moments of ^{20}Na and ^{36}K by β -Radiation
Detected Optical Pumping.
Nuclear Physics A 246 (1975) 187

Deimling, M.;
Optisches Pumpen von ^{80}Rb im Kr-Target.
Messung von Spin und Magnetischem Moment.
Diplomarbeit, Univ. Heidelberg 1975

MATERIALS RESEARCH

Ehrlich, K.; Kaletta, D.;
The Influence of Implanted Helium on Swelling Behaviour and Mechanical
Properties of Vanadium and V-Alloys.
Internat. Conference on Radiation Effects and Tritium Technology for
Fusion Reactors, Gatlinburgh, October 1-3, 1975, AED-CONF-75-498-026

Herschbach, K.; Müller, K.;
Apparatus to Study Irradiation-Induced Creep with a Cyclotron.
Internat. Conference on Radiation Effects and Tritium Technology for
Fusion Reactors,
Gatlinburgh, October 1-3, 1975

NUCLEAR MEDICINE

Meyer, G.J.; Roessler, K.; Stöcklin, G.;
Preparation and Radio Gaschromatographic Identification of
Ortho-, Meta-, Para-Astatochloro-Astatobromo- and Astatiodobenzene
Isomers.
Radiochemical and Radioanalytical Letters, 21 (1975) S. 247-50

Meyer, G.J.; Roessler, K.; Stöcklin, G.;
Zur Reaktivität Anorganischer Formen des Radioelementes ASTAT bei der
Markierung von einfachen aromatischen Systemen und Biomolekülen.
Hauptversammlung der Gesellschaft Deutscher Chemiker, Köln 8.-13. Sept. 1975
AED-CONF-75-404-029

Persigehl, M.; Roessler, K.;
Kinetische Untersuchungen zur Verteilung von anorganischem ^{211}At in gesunden
Mäusen und in Mäusen mit SARKOM 180.
Deutscher Röntgenkongress, Berlin, 1.-3. Mai 1975,
AED-CONF-75-193-078

Helus, F.; Maier-Borst, W.;
Lambrecht, R.M.; Wolf, A.P.;
The Production of Radionuclides ^{123}I , ^{77}Br for Nuclear Medicine with High
Energetic ^4He Particles.
Proc. 7th Int. Conf. on Cyclotrons and their Applications, Birkhäuser, Basel,
1975, p. 474-477

NEUTRON PHYSICS

Cierjacks, S.; Schmalz, G.; Töpke R.; Voß, F.;
Thick Sample Transmission Measurement and Resonance Analysis of the Total
Neutron Cross Section of Iron.
4th Conference on Nucl. Cross Sections and Technology, March 3-7, 1975

Cierjacks, S.; Schmalz, G.; Spencer, R.; Voß, F.; Töpke, R.;
Resonanzanalyse des totalen Neutronenwirkungsquerschnitts von Eisen im
Bereich der intermediären Struktur bei 750 keV.
Frühjahrstagung der DPG, Kernphysik, Den Haag, 7.-11. April 1975,
Verhandlungen der Deutschen Physikalischen Gesellschaft, R.6 Bd. 10 (1975) 828

Cierjacks, S.;
Current Aspects of Nuclear Structure Investigations with Fast Neutrons.
3rd All Union Conf. on Neutron Physics, Kiew, UdSSR, 9.-13. Juni 1975

Töpke, R.; Cierjacks, S.; Voß, F.;
Messung und Resonanzanalyse differentieller elastischer Neutronenstreuquer-
schnitte von ^{40}Ca zwischen 1 und 2.5 MeV.
Frühjahrstagung der DPG, Kernphysik, Den Haag, 7.-11. April 1975,
Verhandlungen der DPG, R.6, Bd. 10 (1975) 829

Voß, F.; Cierjacks, S.; Erbe, D.; Schmalz, G.;
Measurement of the γ -Ray Production Cross Sections from Inelastic Neutron
Scattering in Some Chromium and Nickel Isotopes between 0.5 and 10 MeV
4th Conf. on Nucl. Cross Sections and Techn., Washington, March 3-7, 1975

NUCLEAR CHEMISTRY

Münzel, H.;
Anregungsfunktionen für Kernreaktionen mit geladenen Projektilen.
KFK-Nachrichten, 7 (1975) No. 2, S. 36-38

Bäuerle, W.; Münzel, H.; Krivan, V.;
Optimierung von Massenauflösung und Empfindlichkeit bei der Analyse
durch Vorwärtsstreuung schwerer geladener Teilchen.
KFK-2237 (Dezember 1975)

Wolf, G.K.; Sham, U.; Dreyer, I.;
Chemical Syntheses by Implantation of Ions and Recoil Atoms.
8. Internat. Hot Atom Chemistry Symposium, Spa, May 26-30, 1975

Wolf, G.K.; Römer, J.; Fröschen, W.;
A Method for the Rapid Separation and Identification of Transactinides
with $Z > 103$.
4. Internat. Transplutonium Element Symposium, Baden-Baden, Sept. 13-17, 1975

Wolf, G.K.; Römer, J.; Fröschen, W.; Fritsch, T.; Dreyer, I.;
Chemische Reaktionen in Schmelzen und Festkörpern zur Trennung und
Identifizierung von Schwerionenreaktionsprodukten.
GSI-J2. 74 (November 74) S. 114-24

INSTRUMENTATION AND SYSTEMS DEVELOPMENT

Schatz, G.; Schulz, F.; Schweickert, H.;
Operation of the Karlsruhe Isochronous Cyclotron in 1973 and 1974.
KFK-Ext. 18/75-1

Kappel, W.; Karbstein, W.; Kneis, W.; Möllenbeck, J.; Rämer Ch.;
Schweickert, H.;
Computer-Aided Beam Diagnostics at the Karlsruhe Isochronous Cyclotron.
12. European Cyclotron Progress Meeting, Harwell and Hammersmith,
March 6-8, 1975

Kappel, W.; Karbstein, W.; Kneis, W.; Möllenbeck, J.; Schweickert, H.;
Volk, B.;
Rechnerunterstützte Strahldiagnostik am Karlsruher Isochronzyklotron.
Frühjahrstagung DPG, Kernphysik, Den Haag, 7.-11. April 1975.
Verhandlungen der Deutschen Physikalischen Gesellschaft, R.6 Bd. 10
(1975) S. 706-7

Kappel, W.; Karbstein, W.; Kneis, W.; Möllenbeck, J.;
Schweickert, H.; Volk, B.;
Computer Aided Operation of the Karlsruhe Isochronous Cyclotron
Using CAMAC.
2. Internat. Symposium über CAMAC für Datenverarbeitungsanwendungen,
Brüssel, Oktober 14-16, 1975

Hartwig, D.; Kappel, W.; Kneis, W.; Möllenbeck, J.; Schatz, G.;
Schweickert, H.;
Computer Controlled Beam Diagnostics at the Karlsruhe Isochronous
Cyclotron.
7. Internat. Conference on Cyclotrons and their Applications, Zürich,
August 19-22, 1975

Haushahn, G.; Möllenbeck, J.; Schatz, G.; Schulz, F.; Schweickert, H.;
Status Report of the Axial Injection System at the Karlsruhe Isochronous
Cyclotron.
7. International Conference on Cyclotrons and their Applications,
Zürich, Aug. 19-22, 1975

Bechtold, V.; Friedrich, L.; Finken, D.; Strassner, G.; Ziegler, P.;
Present State of the Karlsruhe Polarized Ion Source.
4. Interat. Symposium on Polarization Phenomena in Nuclear Reactions,
Zürich, August 25-29, 1975

Bechtold, V.; Friedrich, L.; Finken, D.; Strassner, G.; Ziegler, P.;
Polarized Deuterons of a Lambshift Ion Source Accelerated by the
Karlsruhe Isochronous Cyclotron.
7. Interat. Conference on Cyclotrons and their Applications, Zürich,
August 19-22, 1975